



1

2

# **Insight into PM<sub>2.5</sub> Sources by Applying Positive Matrix Factorization (PMF) at an Urban and Rural Site of Beijing**

3

4

5

6

**Deepchandra Srivastava<sup>1</sup>, Jingsha Xu<sup>1</sup>, Tuan V. Vu<sup>1,2</sup>**

7

**Di Liu<sup>1,3</sup>, Linjie Li<sup>3</sup>, Pingqing Fu<sup>4</sup>, Siqi Hou<sup>1</sup>, Zongbo Shi<sup>1,\*</sup>**

8

**and Roy M. Harrison<sup>1†\*</sup>**

9

**<sup>1</sup>School of Geography Earth and Environmental Science, University  
of Birmingham, Birmingham, B15 2TT  
United Kingdom**

10

11

12

13

14

**<sup>2</sup>Now at: School of Public Health, Imperial College London, London  
United Kingdom**

15

16

17

18

19

**<sup>3</sup>Institute of Atmospheric Physics, Chinese Academy of Sciences  
Beijing, 100029, China**

20

21

**<sup>4</sup>Institute of Surface-Earth System Science, Tianjin University,  
Tianjin 300072, China**

22

23

24

25

26

**† Also at: Department of Environmental Sciences / Centre of Excellence in Environmental  
Studies, King Abdulaziz University, PO Box 80203, Jeddah, 21589, Saudi Arabia**

27

28

29

**Corresponding author:** E-mail: [r.m.harrison@bham.ac.uk](mailto:r.m.harrison@bham.ac.uk) (Roy M. Harrison) and  
[z.shi@bham.ac.uk](mailto:z.shi@bham.ac.uk) (Zongbo Shi)

30



31 **ABSTRACT**

32 This study presents the source apportionment of PM<sub>2.5</sub> performed by PMF on data collected at an  
33 urban (Institute of Atmospheric Physics - IAP) and a rural site (Pinggu-PG) in Beijing as part of the  
34 Atmospheric Pollution and Human Health in a Chinese megacity (APHH-Beijing) field campaigns.  
35 The campaigns were carried out from 9<sup>th</sup> November to 11<sup>th</sup> December 2016 and 22<sup>nd</sup> May to 24<sup>th</sup> June  
36 2017. The PMF included both organic and inorganic species, and a seven-factor output provided the  
37 most reasonable solution for the PM<sub>2.5</sub> source apportionment. These factors are interpreted to be  
38 traffic emissions, biomass burning, road dust, soil dust, coal combustion, oil combustion and  
39 secondary inorganics. Major contributors to PM<sub>2.5</sub> mass were secondary inorganics (22-24%),  
40 biomass burning (30-36%), and coal combustion (20-21%) sources during the winter period at both  
41 sites. Secondary inorganics (48%), road dust (20%) and coal combustion (17%) showed the highest  
42 contribution during summer at PG, while PM<sub>2.5</sub> particles were mainly composed of soil dust (35%)  
43 and secondary inorganics (40%) at IAP. Despite this, factors that were resolved based on metal  
44 signatures were not fully resolved and indicate a mixing of two or more sources. PMF results were  
45 also compared with sources resolved from another receptor model (i.e. CMB) and PMF performed  
46 on other measurements (i.e. online and offline aerosol mass spectrometry (AMS)) and showed a good  
47 agreement for some but not all sources. The biomass burning factor in PMF may contain aged aerosols  
48 as a good correlation was observed between biomass burning and oxygenated fractions ( $r^2=0.6-0.7$ )  
49 from AMS. The PMF failed to resolve some sources identified by the CMB and AMS, and appears  
50 to overestimate the dust sources. A comparison with earlier PMF source apportionment studies from  
51 the Beijing area highlights the very divergent findings from application of this method.

52 **Key words:** Source apportionment; PM<sub>2.5</sub>; Beijing; PMF; CMB; online AMS; offline AMS

53



54 **1. INTRODUCTION**

55 Atmospheric particulate matter (PM) is composed of various chemical components and can affect air  
56 quality (and consequently human health), visibility, and ecosystems (Boucher et al., 2013; Heal et  
57 al., 2012). Through absorption and scattering of solar radiation and by affecting clouds, PM also have  
58 a major impact on the climate, and thus the hydrological cycle. PM with an aerodynamic diameter  
59 less than 2.5  $\mu\text{m}$  ( $\text{PM}_{2.5}$ ) is given special attention due to its adverse effects on human health as it can  
60 penetrate deep into human lungs when inhaled. Several recent studies have indicated that many  
61 adverse health outcomes, such as respiratory and cardiovascular morbidity and mortality, are related  
62 to long-term exposure to PM (Lu et al., 2021; Wang et al., 2016; Xing et al., 2016; Xie et al., 2019).  
63 In addition, over a million premature deaths per year are reported in China due to poor air quality  
64 (GBD MAPS Working Group, 2016). Beijing, the capital city of China, is a megacity with  
65 approximately 21 million inhabitants that are regularly exposed to severe haze events. For example,  
66 77 pollution episodes (defined as two or more consecutive days where the average  $\text{PM}_{2.5}$   
67 concentration exceeds  $75 \mu\text{g m}^{-3}$ ) were observed between April 2013 to March 2015 (Batterman et  
68 al., 2016).  $\text{PM}_{2.5}$  concentrations have reached  $1,000 \mu\text{g m}^{-3}$  in some heavily polluted areas of Beijing  
69 (Ji et al., 2014). In addition, a study compared the number of cases of acute cardiovascular,  
70 cerebrovascular, and respiratory diseases in the Beijing Emergency Center and haze data from Beijing  
71 Observatory between 2006 and 2013. Their results showed a rising trend, highlighting the average  
72 number of cases per day for all three diseases was higher on hazy days than on non-hazy days (Zhang  
73 et al., 2015a). Therefore, major control measures were implemented to reduce  $\text{PM}_{2.5}$  pollution in  
74 Beijing (Vu et al., 2019). Recently, one-third of Chinese cities in 2020 were kept under lockdown to  
75 prevent the transmission of COVID-19 virus, which strictly curtailed personal mobility and economic  
76 activities. The lockdown led to an improvement in air quality and managed to bring down the levels  
77 of  $\text{PM}_{2.5}$ . Despite these improvements,  $\text{PM}_{2.5}$  concentrations during the lockdown periods remained  
78 higher than the World Health Organization recommendations, suggesting much further effort is



79 needed (He et al., 2020; Le et al., 2020; Shi et al., 2021). A quantitative source apportionment  
80 provides key information to support such efforts.

81  
82 Receptor models are widely used for source apportionment of PM<sub>2.5</sub>. These methods include positive  
83 matrix factorization (PMF) (Paatero, 1997; Paatero and Tapper, 1994), principal component analysis  
84 (PCA) (Lee et al., 2011), chemical mass balance (CMB) (Watson et al., 1990), and UNMIX (Herrera  
85 Murillo et al., 2012). Among these methods, PMF is a widely used multivariate method that can  
86 resolve the dominant positive factors without prior knowledge of sources. Previous PMF studies,  
87 based on high resolution Aerosol Mass Spectrometer data, have provided valuable information on the  
88 sources of PM in urban Beijing and its surrounding areas (Zhang et al., 2015b; Huang et al., 2010b;  
89 Sun et al., 2010; Sun et al., 2013; Zhang et al., 2013; Zhang et al., 2014; Zhang et al., 2017; Zhang et  
90 al., 2016; Hu et al., 2016; Qiu et al., 2019). However, the factors that influence haze formation and  
91 related sources remain unclear due to its inherent complexity (Tie et al., 2017; Sun et al., 2014). Filter-  
92 based PMF studies provide a valuable tool for identifying sources of airborne particles, by utilising  
93 size-resolved chemical information (Li et al., 2019; Ma et al., 2017a; Tian et al., 2016; Yu et al.,  
94 2013; Song et al., 2007; Song et al., 2006). These source apportionment studies have predominantly  
95 used OC (organic carbon), EC (elemental carbon), water soluble ions and metals as the input data  
96 matrix to explore the co-variances between species and their associated sources, but to the best of our  
97 knowledge, the use of organic markers in PMF has not been explored extensively in Beijing. The use  
98 of organic molecular markers in PMF has enhanced our understanding of the PM fraction as they can  
99 be source specific (Shrivastava et al., 2007; Jaeckels et al., 2007; Zhang et al., 2009; Wang et al.,  
100 2012; Srimuruganandam and Shiva Nagendra, 2012; Schembari et al., 2014; Laing et al., 2015;  
101 Waked et al., 2014; Srivastava et al., 2018) and could potentially offer a clearer link between factors  
102 and sources.

103



104 This study presents the results obtained from the PMF model applied to a filter-based dataset collected  
105 in the Beijing metropolitan area at two sites, urban and rural. The study provides source  
106 apportionment results from both urban and rural locations in Beijing including their temporal and  
107 spatial variations. In addition, the study also presents a short summary of previously published filter-  
108 based studies conducted in the Beijing metropolitan area and their major outcomes. A comparison of  
109 the present PMF results was also made with other source apportionment approaches or applications  
110 of PMF to other datasets, with an aim to discuss the existing PM sources in the Beijing metropolitan  
111 area, including focusing on the strengths and weaknesses of the source apportionment approach  
112 employed.

113

## 114 2. METHODOLOGY

115 Details about the sampling site, measurements, sample collection and analytical procedures are  
116 reported elsewhere (Shi et al., 2019; Xu et al., 2020; Wu et al., 2020), and hence only the essential  
117 information is presented in this section.

118

### 119 2.1 Sampling Site and Sample Collection

120 The PM<sub>2.5</sub> sampling was conducted simultaneously at the urban and rural sites from 9<sup>th</sup> November to  
121 12<sup>th</sup> December 2016 and 22<sup>nd</sup> May to 24<sup>th</sup> June 2017 as part of the Atmospheric Pollution and Human  
122 Health in a Chinese megacity (APHH-Beijing) field campaigns (Shi et al., 2019) (Figure S1). The  
123 urban sampling site (116.39E, 39.98N) - the Institute of Atmospheric Physics (IAP) of the Chinese  
124 Academy of Sciences in Beijing, represents typical condition of central Beijing, there are various  
125 roads nearby including a highway road approximately 200 m away. The rural Pinggu site (PG)  
126 (40.17N, 117.05E) is located in Xibaidian village. This site is approximately 60 km to the north-east  
127 of Beijing city centre and about 4 km north-west of the Pinggu town centre. The site is surrounded



128 by trees and farmland. In addition, residents mainly use coal and biomass for heating and cooking in  
129 individual homes.

130

131 24-hour  $PM_{2.5}$  samples were collected every day on pre-baked quartz filters (Pallflex,  $8 \times 10$  inch) and  
132 47 mm PTFE filters (flow rate of  $15.0 \text{ L min}^{-1}$ ) using high volume (Tisch, USA, flow rate of  $1.1 \text{ m}^3$   
133  $\text{min}^{-1}$ ) and medium volume (Thermo Scientific Partisol 2025i) air sampler. Field blanks were also  
134 collected during the sampling campaign at both sites. The quartz filters were then analyzed for organic  
135 tracers, OC/EC and ion species. PTFE filters were used for the determination of  $PM_{2.5}$  mass and  
136 metals. Details on preparation and conservation of these filter samples have already been reported  
137 elsewhere (Wu et al., 2020; Xu et al., 2020).

138

139 Real time composition of non-refractory  $PM_1$  particles (NR- $PM_1$ ) was measured using an Aerodyne  
140 aerosol mass spectrometer (AMS) at a time resolution of 2.5 min. The operational details on the AMS  
141 measurements have been given elsewhere (Xu et al., 2019). In addition, the measurements of gaseous  
142 species such as  $O_3$ , CO, NO,  $NO_2$  and  $SO_2$  were performed using gas analyzers. The meteorological  
143 parameters including temperature (T), relative humidity (RH), wind speed (WS), and wind direction  
144 (WD) were also measured at both sites.

145

## 146 **2.2 Analytical Procedure**

147 In all 62 and 72 chemical species were quantified in each  $PM_{2.5}$  sample from IAP and PG,  
148 respectively. This included EC/ OC, 36 organic tracers, 7 major inorganic ions ( $Na^+$ ,  $K^+$ ,  $Ca^{2+}$ ,  $NH_4^+$ ,  
149  $Cl^-$ ,  $NO_3^-$  and  $SO_4^{2-}$ ) and 17 metallic elements (V, Cr, Co, Mn, Ni, Cu, Zn, As, Br, Sr, Ag, Cd, Sn,  
150 Sb, Ba, Hg and Pb) at IAP. Similarly, the identified species at PG included EC/OC, 51 organic tracers,  
151 7 major inorganic ions and 12 metallic elements (V, Cr, Co, Mn, Ni, Cu, Zn, As, Sr, Sb, Ba, and Pb).  
152 EC and OC measurements were performed using a Sunset lab analyser (model RT-4) and DRI multi-



153 wavelength thermal-optical carbon (model 2015) analyser based on the EUSAAR2 (European  
154 Supersites for Atmospheric Aerosol Research) transmittance protocol at both sites, IAP and PG,  
155 respectively, following the procedure explained by Paraskevopoulou et al. (2014). Major inorganic  
156 ions and metallic elements were analysed using an ion chromatograph (Dionex, Sunnyvale, CA,  
157 USA) and Inductively coupled plasma-mass spectrometer (ICP-MS) at both sites, respectively. Major  
158 crustal elements including Al, Si, Ca, Ti and Fe were determined by X-ray fluorescence spectrometer  
159 (XRF).

160  
161 Organic tracers at IAP included n-alkanes 11 C<sub>24</sub>-C<sub>34</sub>, 2 hopanes, 17 PAHs, 3 anhydrous sugars  
162 (levoglucosan, mannosan, galactosan), 2 fatty acids (palmitic acid, stearic acid) and cholesterol.  
163 These organic tracers were analysed by gas chromatography mass spectrometry (GC/MS, Agilent  
164 7890A GC plus 5975C mass-selective detector) coupled with a DB-5MS column (30 m × 0.25 mm ×  
165 0.25 μm) following the protocol explained in Xu et al. (2020). At PG, organic tracers were analysed  
166 based on the method reported by Wu et al. (2020) using GC/MS (Agilent GC-6890N plus MSD-  
167 5973N) coupled with a HP-5MS column (30 m × 0.25 mm × 0.25 μm). This included quantification  
168 of similar species (12 n-alkanes C<sub>24</sub>-C<sub>35</sub>, 9 hopanes, 22 PAHs, 3 anhydrous sugars (levoglucosan,  
169 mannosan, galactosan), 4 fatty acids (palmitic acid, stearic acid, linoleic acid, oleic acid) and  
170 cholesterol) with few additional ones. Recoveries for the identified organic tracers ranged from 70-  
171 100% and 80-110 %, at IAP and PG, respectively. Field blank were also analysed as part of quality  
172 control and demonstrated very low contamination (<5%).

173  
174 In addition, one or two punches of PM<sub>2.5</sub> filter sample were also analysed offline using AMS to  
175 investigate the water-soluble OA (WSOA) mass spectra following the procedure explained  
176 previously (Qiu et al., 2019).

177



## 178 2.4 Positive Matrix Factorization

179 Detailed information on the receptor modelling methods used within this study can be found  
180 elsewhere (Paatero and Tapper, 1994; Hopke, 2016). Positive matrix factorization (PMF) is a  
181 multivariate factor analysis tool and based on a weighted least square fit, where the weights are  
182 derived from the analytical uncertainty. The best model solution was obtained by minimizing  
183 residuals obtained between modeled and observed input species concentrations Estimation of  
184 analytical uncertainties for the filter-based measurements was calculated using Eq. (1) (Polissar et al.,  
185 1998).

$$186 \sigma_{ij} = \begin{cases} \frac{5}{6} LD_j & \text{if } X_{ij} < LD_j \\ \sqrt{(0.5 * LD_j)^2 + (EF_j X_{ij})^2} & \text{if } X_{ij} \geq LD_j \end{cases} \quad \text{Eq. (1)}$$

188 where  $LD_j$  is the detection limit for compound  $j$  and  $EF_j$  is the error fraction for the compound  $j$ . The  
189 detection limits of all compounds used in the PMF model is given in Table S1 (SI). The U.S.  
190 Environmental Protection Agency (US-EPA) PMF 5.0 software was used in this work to perform the  
191 source apportionment.  
192

193  
194 **Selection of the input data.** The selection of species used as input data for the PMF analysis is  
195 important and can significantly influence the model results (Lim et al., 2010). The following set of  
196 criteria were used for the selection of the input species: signal to noise ratio (S/N) (Paatero and Hopke,  
197 2003), major PM chemical species, compounds with maximum data points above the detection limit  
198 and those being considered as specific markers of a given source (e.g., levoglucosan, picene) (Oros  
199 and Simoneit, 2000; Simoneit, 1999) were selected. These steps were taken to limit the input data  
200 matrix according to the total number of samples (n=133); some species were also not included if they  
201 belonged to a single source and correlated with another marker of this source. A total of 31 species  
202 were used in the model (PM<sub>2.5</sub>, OC, EC, K<sup>+</sup>, Na<sup>+</sup>, Ca<sup>2+</sup>, NH<sub>4</sub><sup>+</sup>, NO<sub>3</sub><sup>-</sup>, SO<sub>4</sub><sup>2-</sup>, Cl<sup>-</sup>, Ti, V, Mn, Ni, Zn, Pb,



203 Cu, Fe, Al, C26, C29, C31, 17 $\alpha$ (H)-22,29,30-trisnorhopane, 17 $\beta$ (H), 21 $\alpha$ (H)-30-norhopane, chrysene,  
204 benzo(b)fluoranthene, benzo(a)pyrene, picene, corene, levoglucosan, and stearic acid). The  
205 concentration of PM<sub>2.5</sub> was included as a total variable in the model (with large uncertainties) to  
206 directly determine the source contributions to the daily mass concentrations.

207  
208 ***Selection of the final solution.*** As normally recommended, a detailed evaluation of factor profiles,  
209 temporal trends, fractional contribution of major species to each factor and correlations with external  
210 tracers, were investigated carefully to select the appropriate number of factors.

211  
212 A few constraints were also applied to the base run to obtain clearer chemical source profiles in the  
213 final solution. The general framework for applying constraints to PMF solutions has already been  
214 discussed elsewhere (Amato et al., 2009; Amato and Hopke, 2012). The changes in the  $Q$  values were  
215 considered here as a diagnostic parameter to provide insight into the rotation of factors. All model  
216 runs were carefully monitored by examining the  $Q$  values obtained in the robust mode. To limit  
217 change in the  $Q$ -value, only “soft pulling” constraints were applied. The change in the  $Q$ -robust was  
218  $< 1\%$ , which is acceptable as per PMF guidelines ( $< 5\%$ ) (Norris et al., 2014). Finally, three criteria  
219 were used to select the optimal solution, including correlation coefficient ( $r$ ) between the measured  
220 and modelled species, bootstrap and t-test (two-tailed paired t-test) performed on the base and  
221 constraint runs, as explained previously (Srivastava et al., 2018).

222

## 223 **2.5 Back trajectories and Geographical Origins**

224 The geographical origin of selected identified sources and pollutants was investigated using  
225 concentration-weighted trajectory (CWT), non-parametric wind regression (NWR), and cluster  
226 analysis methods. NWR combines ambient concentrations with co-located measurements of wind  
227 direction and speed and highlights wind sectors that are associated with high measured concentrations  
228 (Henry et al., 2009). The general principle is to smooth the data over a fine grid, so that a weighted



229 concentration could be estimated by any wind direction ( $\phi$ )/wind speed ( $v$ ) couple, where the  
230 weighing coefficients are determined through Gaussian-like functions. CWT and cluster analysis  
231 assess the potential transport of pollution over large geographical scale (Polissar et al., 2001). These  
232 approaches combine atmospheric concentrations measured at the receptor site with back trajectories  
233 and residence time information and help to geographically evaluate air parcels responsible for high  
234 concentrations. For this purpose, hourly 24-h back trajectories arriving at 200 m above sea level were  
235 calculated from the PC-based version of HYSPLIT v4.1 (Stein et al., 2015; Draxler, 1999). NWR,  
236 CWT calculations and cluster analysis, were performed using the ZeFir Igor package (Petit et al.,  
237 2017).

238

## 239 **2.6 Other Receptor Modelling Approaches**

240 Sources were also resolved at both sites separately using another receptor model known as chemical  
241 mass balance (CMB) as well as PMF performed on high resolution AMS data collected at IAP. Details  
242 on sources resolved using these approaches are reported elsewhere (Wu et al., 2020; Xu et al., 2020;  
243 Sun et al., 2020).

244

245 Briefly, CMB is based on a linear least squares approach and accounts for uncertainties in both, source  
246 profiles and ambient measurements to apportion the sources of OC. The US EPA CMB8.2 software  
247 was used for this purpose at both sites. The source profiles applied in the model were taken from local  
248 studies to better represent the sources, including profiles of straw burning (Zhang et al., 2007), wood  
249 burning (Wang et al. 2009), gasoline and diesel vehicles (Cai et al. 2017), industrial and residential  
250 coal combustion (Zhang et al., 2008), and cooking (Zhao et al., 2015). Only the source profile for  
251 vegetative detritus (Rogge et al. 1993; Wang et al., 2009) was not available from local studies. The  
252 selected fitting species included EC, anhydrous sugar (levoglucosan), fatty acids, PAHs, hopanes and  
253 alkanes



254 **3. RESULTS AND DISCUSSION**

255 **3.1 Overview on PM Sources in Beijing based on the Current Source Apportionment Study**

256 A seven-factor output provided the most reasonable solution for the PM<sub>2.5</sub> source apportionment  
257 performed on the combined dataset from IAP and PG (Figures 1 and 2).

258

259 Based on the factor profiles, we identified traffic emissions, biomass burning, road dust, soil dust,  
260 coal combustion, oil combustion and secondary inorganics. For the same dataset, solutions with six  
261 sources were less explanatory and some factors were mixed. Conversely, an increase in the number  
262 of factors led to the split of meaningful factor profiles. In the final solution, the comparison of the  
263 reconstructed PM<sub>2.5</sub> contributions from all sources with measured PM<sub>2.5</sub> concentrations for different  
264 seasons at both sites showed good mass closure ( $r^2 = 0.61-0.91$ , slope = 0.99-1.12,  $p < 0.05$ , ODR  
265 (orthogonal distance regression)). A low  $r^2$  (0.61) value was observed for the summer period at IAP  
266 (Figure S2). This may be due to the inability of PMF to model low concentrations observed for  
267 sources such as biomass burning and coal combustion during the summer. In addition, most of the  
268 species showed good agreement with measured concentrations (Table S2). Bootstrapping on the final  
269 solution showed stable results with more than 95 out of 100 bootstrap mapped factors (Table S3).  
270 Finally, no significant difference ( $p > 0.05$ ) was observed in the factor chemical profiles between the  
271 base and the constrained runs (Table S4).

272

273 Overall, secondary inorganics, biomass burning, and coal combustion sources were the main  
274 contributors to the total PM<sub>2.5</sub> mass during winter (Figure 3). These sources accounted for 22%, 36%,  
275 20%, and 24%, 30%, 21% of PM<sub>2.5</sub> mass at IAP and PG, respectively. Secondary inorganics, road  
276 dust and coal combustion showed the highest contribution during summer at PG, while PM<sub>2.5</sub> particles  
277 were mainly composed of soil dust and secondary inorganics at IAP. Identified aerosol sources, factor  
278 profiles and temporal evolutions are discussed below. Note, PMF was carried out on the combined  
279 datasets and thus only provides a single set of factor profiles for both sites. Similar to previous studies



280 (Li et al., 2019; Ma et al., 2017a; Tian et al., 2016; Yu et al., 2013; Liu et al., 2019; Zhang et al.,  
281 2013), neither secondary organic aerosol nor cooking emissions were identified, and given the good  
282 mass closure must be present within other source categories.

283  
284 **Coal combustion.** Coal combustion was identified based on it accounting for a high proportion of  
285 PAHs (27-78%), especially picene (78%) as a specific marker of coal combustion (Oros and  
286 Simoneit, 2000), together with significant amount of OC (45%) and EC (29%) (Figure 1). This factor  
287 also made a substantial contribution to n-alkanes (28-58%), stearic acid (64%) and hopanes (53-56%),  
288 as these compounds are also abundant in coal smoke (Bi et al., 2008; Zhang et al., 2008; Oros and  
289 Simoneit, 2000; Guo et al., 2015).

290  
291 The coal combustion factor accounted for 20% of the PM mass ( $16.0 \mu\text{g m}^{-3}$ ) at the urban site IAP  
292 during winter and followed typical seasonal variations. However, the contributions of this source to  
293 PM<sub>2.5</sub> mass were broadly similar (21% vs 17%, Figure 3) at PG during both seasons, while the average  
294 concentrations were higher in winter than summer ( $19.4 \mu\text{g m}^{-3} > 4.6 \mu\text{g m}^{-3}$ ). Due to a lack of  
295 infrastructure at the rural site PG, the residents still use coal for cooking and heating purposes at the  
296 time of sampling (Shi et al., 2019). There is a reduction in coal usage for heating due to elevated  
297 temperatures in the summertime, leading to low levels of this factor. But the similar contribution at  
298 the rural site could be linked to consistent cooking activities throughout the year (Figure 2) (Shi et  
299 al., 2019; Tao et al., 2018). These results were in good agreement with previous observations reported  
300 at the same urban site (18%) (Ma et al., 2017a; Tian et al., 2016). In addition, similar contributions  
301 were also observed at other urban locations around Beijing (Wang et al., 2008; Liu et al., 2019).

302  
303 This factor also included significant contributions from levoglucosan (60%). Levoglucosan, a major  
304 pyrolysis product of cellulose, and has been proposed as molecular marker of biomass burning  
305 aerosols (Simoneit, 1999). A study conducted in China suggested that residential coal combustion  
306 can also contribute significantly to levoglucosan emissions, based on both source testing and ambient



307 measurements (Yan et al., 2018). Therefore, it is expected that the contribution of levoglucosan is  
308 probably linked to residential coal use for cooking in this case. It is also possible that the high  
309 contribution of levoglucosan could also be linked to model bias as the PMF model only provides an  
310 average factor profiles for both sites irrespective of their nature (rural vs. urban) and different  
311 sampling periods (summer vs. winter).

312  
313 This was further supported as NWR and CWT analysis showed similar results, mostly dominated by  
314 a northerly flow during the winter period at both sites. High concentrations of this source and  
315 levoglucosan were observed at low wind speeds (Figure S3), indicating the significant role of local  
316 activities. Higher levels were observed at the rural site PG ( $19.4 \mu\text{g m}^{-3}$  vs  $16.0 \mu\text{g m}^{-3}$  at the urban  
317 site). However, a south-westerly flow was dominant during summer and could be related to transport  
318 of air masses from the Hebei province where a large number of industries operate.

319  
320 **Oil combustion.** The oil combustion factor profile included high contributions to V (79%) and Ni  
321 (70%) (see Figure 1). V and Ni are widely used markers for oil combustion in residential, commercial  
322 and industrial applications (Viana et al., 2008; Mazzei et al., 2008; Pant et al., 2015; Huang et al.,  
323 2021). The V/Ni ratio obtained in this study was 0.9, close to the previously obtained ratio for residual  
324 oil used in power plants (Swietlicki and Krejci, 1996). Results suggest this source might be attributed  
325 to residual oil combustion linked to industrial activities as a large number of highly polluting  
326 industries are still located in the Beijing neighbourhood (Li et al., 2019). CWT and NWR analysis  
327 suggested the influence of regional transport at both sites, highlighting the dominance of south  
328 westerly and south easterly flows during the winter and summer at both sites (Figure S4).

329  
330 The source did not show any seasonal pattern (Figure 2), and accounted for 2% ( $1.4 \mu\text{g m}^{-3}$ ) and 6%  
331 ( $1.6 \mu\text{g m}^{-3}$ ) at IAP, and 8% ( $7.1 \mu\text{g m}^{-3}$ ) and 9% ( $2.1 \mu\text{g m}^{-3}$ ) at PG of the  $\text{PM}_{2.5}$  mass during winter  
332 and summer, respectively (Figure 3). The contribution of this source to the PM mass was within the



333 similar range to the previous study conducted at the same urban site (contribution 4.7%) (Li et al.,  
334 2019), which also found a high proportion of V attributed to the identified source.

335  
336 **Biomass burning.** The biomass burning factor was characterized by high contributions to  $\text{Cl}^-$  (74%),  
337  $\text{K}^+$  (27%) and levoglucosan (25%) (Figure 1). This factor also made significant contributions to PAHs  
338 (Chry (66%), B[b]F (66%), Cor (68%)) and followed a clear seasonal variation with a higher  
339 contribution in winter (Figure 2). It accounted for 36 % ( $29.0 \mu\text{g m}^{-3}$ ) and 30% ( $27.3 \mu\text{g m}^{-3}$ ) of the  
340  $\text{PM}_{2.5}$  mass during the wintertime at IAP and PG, respectively (Figure 3), while the contribution  
341 during the summertime was extremely low. This was expected due to elevated temperature during  
342 the summer period and reduction in biomass burning activities. In addition,  $\text{NO}_3^-$  (24%), and  $\text{NH}_4^+$   
343 (24%) also contributed significantly to the biomass burning factor. Biomass burning is an important  
344 natural source of  $\text{NH}_3$  (Zhou et al., 2020) which rapidly reacts with  $\text{HNO}_3$  to form  $\text{NH}_4\text{NO}_3$  aerosols.  
345 The presence of  $\text{NH}_4\text{NO}_3$  aerosols in biomass burning plumes, has also been reported previously  
346 (Paulot et al., 2017; Zhao et al., 2020).

347  
348 It was unexpected to observe a low contribution of levoglucosan, a known biomass burning marker,  
349 to this factor. However, model bias and the contribution of other relevant sources to levoglucosan  
350 could cause such observations, as discussed above.  $\text{K}^+$  is also produced from the combustion of wood  
351 lignin and has been used extensively as an inorganic tracer to apportion biomass burning contributions  
352 to ambient aerosol (Zhang et al., 2010; Lee et al., 2008b). However, the contribution of  $\text{K}^+$  to this  
353 factor was not relatively low, possibly because  $\text{K}^+$  has also other sources, such as soil dust (Duvall et  
354 al., 2008).  $\text{Cl}^-$  can be emitted from both coal combustion and biomass burning, especially during the  
355 cold period in Beijing (Sun et al., 2006). It is also important to note that high  $\text{Cl}^-$  levels observed in  
356 this factor could be associated with coal combustion as  $\text{Cl}^-$  has been used to represent coal combustion  
357 activities in China (Wang et al., 2008). If we consider this, high  $\text{Cl}^-$  levels related to the coal  
358 combustion factor should have also shown a significant contribution to PM mass during the



359 summertime at the rural site (PG) as residents near the rural site mostly use coal and biomass for  
360 cooking activities as discussed above, but they do not. Results suggest this factor can be attributed  
361 mainly to biomass burning aerosols in the Beijing metropolitan area, but some influence of coal  
362 combustion signals cannot be ignored. Back trajectory analysis also confirmed the local origin of this  
363 source during the wintertime at both sites (Figure S5).

364

365 The source contribution reported in the present study was higher than that found in earlier studies in  
366 Beijing (11-20%) (Li et al., 2019; Ma et al., 2017a; Tian et al., 2016; Yu et al., 2013; Song et al.,  
367 2007; Song et al., 2006; Liu et al., 2019), suggesting some inclusion of coal burning. As both these  
368 sources follow a similar typical seasonal variation, i.e., high concentration during the cold period, it  
369 makes their separation difficult due to correlation.

370

371 **Secondary inorganics.** Secondary inorganics were typically characterized by high contributions to  
372  $\text{NO}_3^-$ ,  $\text{SO}_4^{2-}$  and  $\text{NH}_4^+$  (55%, 56% and 56% of the total species mass, respectively) (Figure 1). This  
373 factor showed a temporal variation, with remarkably high concentrations observed during the period  
374 of high relative humidity (RH) and low ozone concentration in the winter (Figure S6). The  
375 heterogeneous reactions on pre-existing particles in the polluted environment under high RH and low  
376 ozone conditions have been shown to play a key role in the formation of secondary aerosols compared  
377 to gas-phase photochemical processes (Sun et al., 2013; Niu et al., 2016; Ma et al., 2017b). Therefore,  
378 aqueous phase processes may be the major formation pathway for secondary inorganic aerosols in  
379 Beijing during the study period. Additionally, the factor showed a similar contribution (22-24%) to  
380 PM mass in winter at both sites. This value is lower than the value reported at the other urban location  
381 (44%) in Beijing as a part of same campaign (Liu et al., 2019), although it should be noted that the  
382 sampling site and dates differed.

383



384 The highest contribution to the PM mass was observed during the summertime, with an average  
385 concentration of  $11.1 \mu\text{g m}^{-3}$  (40%) and  $13.2 \mu\text{g m}^{-3}$  (48%) at IAP and PG, respectively (Figure 3).

386  
387 **Traffic emissions.** The traffic emissions factor showed relatively high contributions to metallic  
388 elements, such as Zn (47%), Pb (57%), Mn (27%) and Fe (22%) (Figure 1). Zn is a major additive to  
389 lubricant oil. Zn and Fe can also originate from tyre abrasion, brake linings, lubricants and corrosion  
390 of vehicular parts and tailpipe emission (Pant and Harrison, 2012; Pant and Harrison, 2013;  
391 Grigoratos and Martini, 2015; Piscitello et al., 2021). As the use of Pb additives in gasoline has been  
392 banned since 1997 in Beijing, the observed Pb emissions may be associated with wear (tyre/brake)  
393 rather than fuel combustion (Smichowski et al., 2007). These results suggest the contribution of both  
394 exhaust and non-exhaust traffic emissions to this factor. Further insight on the type of non-exhaust  
395 emissions is hard to predict as these metal concentrations vary according to several parameters, such  
396 as traffic volume and patterns, vehicle fleet characteristics and the climate and geology of the region  
397 (Duong and Lee, 2011).

398  
399 Traffic sources accounted for 9% and 6% of  $\text{PM}_{2.5}$  mass during the winter and summertime at IAP  
400 (Figure 3), corresponding to an average concentration of  $7.4 \mu\text{g m}^{-3}$  and  $1.8 \mu\text{g m}^{-3}$ , respectively. In  
401 addition, a low contribution (4%) was observed at PG during both seasons as PG experiences a low  
402 traffic volume. The contribution of the traffic source to the  $\text{PM}_{2.5}$  mass was found to be low compared  
403 to other studies conducted in the Beijing area; (14-20%) (Li et al., 2019; Tian et al., 2016; Yu et al.,  
404 2013; Liu et al., 2019), with the exception of a study by Ma et al. (2017a) where a similar contribution  
405 was reported. The observed low contribution was further supported as a recent study also confirms  
406 that road traffic remains a dominant source of  $\text{NO}_x$  and primary coarse PM, however, it only accounts  
407 a relatively small fraction of  $\text{PM}_{2.5}$  mass at urban locations in Beijing (Harrison et al., 2021). It should  
408 be noted that nitrate that can be formed from  $\text{NO}_x$  emitted from road traffic is not included in this  
409 factor. Despite the low factor contribution, the resolved chemical profile of this source was consistent  
410 with previously identified profiles linked to road traffic emissions in the Beijing area (Ma et al.,



411 2017a; Yu et al., 2013). We noticed that OC/EC contribution in this factor is relatively low, while it  
412 may be higher in traffic emissions. However, given the modern gasoline fleet in Beijing (Jing et al.,  
413 2016), it is not unexpected to observe low OC and EC contribution. We do expect higher OC and EC  
414 contribution from diesel vehicles. In addition, there was no obvious seasonal variation as expected,  
415 though slightly higher concentrations were observed in the cold period, probably due to the typical  
416 atmospheric dynamics, and consequent poorer dispersion at this time of year.

417  
418 Metallic elements such as Mn, Fe and Zn were also used previously to indicate industrial activities  
419 (Li et al., 2017; Yu et al., 2013). Back trajectory analysis reveals the influence of local emissions with  
420 a slight regional transport during the winter period at both sites, dominated by north easterly flow  
421 (Figure S7). Therefore, there is a possibility that these elements could also come from the Hebei  
422 province where a large number of smelter industries are located. North-easterly and south-easterly  
423 flows were dominant during the summer period at IAP and PG with possible regional influence. These  
424 observations suggest that indeed this factor contains traffic aerosols, though a significant influence  
425 of industrial emissions cannot be ruled out.

426  
427 **Road dust.** This factor makes a major contribution to crustal species, such as Na<sup>+</sup>, Al and Fe (60%,  
428 48% and 34% of species in this factor respectively) suggesting this factor may represent the  
429 characteristics of a dust related source as reported previously (Kim and Koh, 2020). In addition, the  
430 given factor also included significant contributions to Mn, Pb and Zn (26%, 23% and 20% of species  
431 in this factor respectively), which are associated with brake and tyre wear as mentioned above (Pant  
432 and Harrison, 2012; Pant and Harrison, 2013; Grigoratos and Martini, 2015; Piscitello et al., 2021).  
433 High concentrations of Zn and Pb have also been reported for particles emitted from asphalt pavement  
434 (Canepari et al., 2008; Sörme et al., 2001). In addition, the ratio of Fe/Al observed in the factor  
435 chemical profile was 1.26, much higher than the value observed in the earth's crust (0.6), suggesting  
436 an anthropogenic origin of some Fe (Sun et al., 2005). This is likely as processes associated with  
437 vehicles, such as tyre/brake wear and road abrasion, can contaminate soil with metals, as the urban



438 sampling site is located close to roads suggesting the resolved factor is likely linked to road dust  
439 emissions. These metals (Fe and Al) can also have industrial sources as already reported in the Beijing  
440 area (Wang et al., 2008; Tian et al., 2016; Yu et al., 2013; Li et al 2019). The Beijing-Tianjin-Hebei  
441 region is the largest urbanised megalopolis region in northern China, and home to many iron and steel  
442 making industries. Fe is characteristic components of iron and steel industry emissions (Li et al.,  
443 2019) while Al may also come from metal processing (Yu et al., 2013). However, disentangling the  
444 influence of industrial emissions would require further investigation.

445  
446 This source also made significant contributions to OC, EC and  $\text{SO}_4^{2-}$  (11-19%) (Figure 1) and was  
447 consistent with the road dust source profiles observed previously in the Beijing area (Song et al.,  
448 2006; Song et al., 2007; Tian et al., 2016; Yu et al., 2013). This factor accounted for 20% of the  $\text{PM}_{2.5}$   
449 mass during the summertime ( $5.5 \mu\text{g m}^{-3}$ ) with exceptionally low contribution (3%) during the cold  
450 period at PG (Figure 3). However, the factor contribution at IAP was similar during both seasons. In  
451 addition, the contribution to PM mass at IAP in this study was similar to that reported by Tian et al.  
452 (2016) and the studied urban site in both cases was the same. Crustal dust mass was also estimated  
453 based on the concentrations of Al, Si, Fe, Ca, and Ti using the equation below (Chan et al., 1997).

$$454 \quad \text{Crustal dust} = 1.16(1.9\text{Al} + 2.15\text{Si} + 1.41\text{Ca} + 1.67\text{Ti} + 2.09\text{Fe})$$

455  
456 Good correlation was observed between the estimated crustal dust and this factor during both seasons  
457 at PG (rural, winter:  $r^2 = 0.78$ ,  $m(\text{slope}) = 0.9$ ; summer:  $r^2 = 0.94$ ,  $m = 0.5$ ) and IAP (urban, winter:  $r^2$   
458  $= 0.51$ ,  $m = 1.3$ ; summer:  $r^2 = 0.68$ ,  $m = 1.2$ ), highlighting that this may also contain a significant  
459 fraction of crustal dust (Figure S8). This suggests the identified factor is not resolved cleanly and  
460 contains a mixed characteristic of road dust and crustal dust.

461  
462 **Soil dust.** This factor mainly represents wind-blown soils and was typically characterized by a high  
463 contribution to crustal elements, such as Ti (63%),  $\text{Ca}^{2+}$  (41%), Fe (27%) and Al (17%) (Figure 1).



464 In addition, the contributions to Mn and Zn in the factor profile (Mn=24%, Zn=15%) suggest that the  
465 given source also included resuspended road dust but probably to a lesser extent. No clear seasonal  
466 variation was observed. This source also showed a significant contribution to n-alkanes (e.g., C29,  
467 C31), derived from epicuticular waxes of higher plant biomass (Kolattukudy, 1976; Eglinton et al.,  
468 1962), with the highest contribution (37%) to C31. This suggests the presence of plant derived organic  
469 matter in the soil dust, which is also consistent with a high contribution to OC (15%).

470  
471 The factor showed a high contribution (35%,  $9.8 \mu\text{g m}^{-3}$ ) to  $\text{PM}_{2.5}$  mass during the summertime at  
472 IAP, while the contribution during other seasons at both sites was less than 10% (Figure 3). The factor  
473 profile resolved here was similar to the profile reported by Ma et al. (2017a) for soil dust, but their  
474 soil dust factor only showed a 10 % contribution to  $\text{PM}_{2.5}$  mass. In addition, other previous studies  
475 (Yu et al., 2013; Zhang et al., 2013) also reported significant contribution of soil dust to  $\text{PM}_{2.5}$  mass,  
476 suggesting that soil dust is an important contributor to  $\text{PM}_{2.5}$  mass in the Beijing area. It is also  
477 expected as Beijing is in a semi-arid region and there are sparsely vegetated surfaces both within and  
478 outside the city. This factor also showed good agreement with the crustal fraction estimated from the  
479 element masses only during winter at PG ( $r^2 = 0.51$ ) and summer at IAP ( $r^2 = 0.58$ ). This again  
480 highlights the probable mixing of this source with other factors, or mis-attribution. Back trajectory  
481 analysis also indicates the influence of regional transport during the summer period at IAP, dominated  
482 by south easterly-westerly flow (Figure S9) due to high windspeeds ( $3.6 \text{ m s}^{-1}$ ). Therefore, there is a  
483 possibility that the high contribution is linked to long-range transport in advected air masses. A recent  
484 study (Gu et al., 2020) conducted in Beijing showed the high concentrations of more oxidised aerosols  
485 during summer due to enhanced photochemical processes; however, such type of source was not  
486 resolved due to a lack of filter based markers. This suggests the given source may contain some  
487 influence from an unidentified/unresolved SOC fraction. Although the most plausible attribution  
488 appears to be to soil dust, it is not fully resolved from other sources.

489



490 The use of Si in PMF could provide a better understanding on these dust related sources. However, it  
491 is not used in the present PMF input due to high number of missing data points. The sensitivity of  
492 PMF results to the use of Si has also been investigated by adding Si to the input matrix and providing  
493 high uncertainty to the missing data. No change was observed in the factor profile and temporal  
494 variation of the resolved factors compared to the present one. In addition, we also noticed a good  
495 correlation between Si and Al, where Al has been used in PMF (Figure S10). Several PMF runs were  
496 also made with inorganic data only, however the resolved factors were either mixed or hard to  
497 identify. In addition, attempts to improve the PMF results by varying the input species and by  
498 analysing data for the IAP and PG sites separately did not offer any advantage.

499  
500 **3.2 Comparison of Filter-Based PMF Results with other Receptor Modelling Approaches**  
501 **on the same Dataset**

502 The source apportionment results from PMF were compared with those from CMB on the same filter-  
503 based composition data and PMF performed on other measurements (i.e. online AMS (PM<sub>1</sub>), offline  
504 AMS (PM<sub>2.5</sub>)) to get a deeper insight into the identified PMF factors and their origins (Figs. 4, 5, 6,  
505 7). The CMB method resulted in the estimation of eight OC sources (i.e., vegetative detritus,  
506 residential coal combustion (CC), industrial CC, cooking, diesel vehicles, gasoline vehicles, biomass  
507 burning, other OC), including one secondary factor (Other OC) at both sites (IAP and PG) The online  
508 AMS datasets allowed the identification of 6 OA (MOOOA (more oxidised oxygenated OA),  
509 LOOOA (low more oxidised oxygenated OA), OPOA (oxidised primary OA), BBOA (biomass  
510 burning OA), COA (cooking OA), CCOA (coal combustion OA) factors during winter at IAP, while  
511 analyses on the offline AMS measurements resolved 4 OA (OOA, BBOA, COA, CCOA) factors.

512  
513 For these analyses, OC concentrations related to the online/offline AMS OA factors were further  
514 calculated by applying OC-to-OA conversion factors specific to each source, i.e., 1.35 for coal  
515 combustion organic carbon (Sun et al., 2016), 1.38 for cooking organic carbon, 1.58 for biomass



516 burning organic carbon (Xu et al., 2019), and 1.78 for the oxygenated fraction (Huang et al., 2010a)  
517 and used to evaluate the OC concentrations of relevant OA factors.

518  
519 Only OC equivalent concentrations were used to perform comparison for all approaches. OC mass  
520 closure was also verified at IAP during the wintertime by investigating the relation between: OC  
521 modelled by online AMS PMF vs filter based PMF ( $r^2=0.7$ , slope=1.17), OC measured vs OC  
522 modelled by filter based PMF ( $r^2=0.7$ , slope=1.07), OC measured vs OC modelled by online AMS  
523 PMF ( $r^2=0.9$ , slope=0.92), OC modelled by offline AMS PMF vs OC model by filter based PMF  
524 ( $r^2=0.6$ , slope=0.75), OC measured vs OC modelled by offline AMS PMF ( $r^2=0.9$ , slope=1.41), and  
525 OC measured vs WSOA (offline AMS) ( $r^2=0.9$ , slope=0.85) (Figure S11). The comparison of OC  
526 modelled by PMF and CMB was also investigated at IAP ( $r^2=0.8$ , slope=1.05) and PG ( $r^2=0.6$ ,  
527 slope=1.78) (Figure S12). All source apportionment approaches showed a fairly good agreement in  
528 reconstructing the total OC mass, justifying their direct comparison. In addition, it should be noted  
529 that the difference in the sampling size cut-off between online AMS (NR-PM<sub>1</sub>) and filter  
530 measurements (PM<sub>2.5</sub>) may contribute to the differences observed in the source apportionment  
531 results. Therefore, we also compared the relation between NR-PM measured vs PM measured  
532 ( $r^2=0.96$ , slope=0.92), and NR-PM measured vs PM modelled by filter based PMF ( $r^2=0.9$ ,  
533 slope=1.29) (Figure S13). The agreements observed suggest that the most of the PM<sub>2.5</sub> mass was  
534 accounted for by the PM<sub>1</sub> fraction, indicating that the difference in the size-cut off is relatively small.

535

#### 536 (a) With CMB results at IAP

537 Resolved CMB and PMF factors were compared including data from both seasons at IAP and PG  
538 (Figure 4). A good correlation ( $r^2=0.6$ ,  $n=68$ ,  $p<0.05$ ) was observed between biomass burning factors,  
539 suggesting that this source was well resolved using both approaches (Figure 4). However, a slightly  
540 higher concentration was reported by the CMB model (2.0 and 1.6  $\mu\text{g m}^{-3}$  by CMB and PMF  
541 respectively). Individual coal combustion factors (industrial/residential) did not show any



542 significant correlation ( $r^2 < 0.2$ ) with the coal combustion factor identified using PMF, although the  
543 total coal combustion fraction from CMB, the sum of industrial and residential fractions, did show  
544 an improved correlation ( $r^2 = 0.4$ ). Some improvement on the correlation was seen if two outlier  
545 datapoints were removed (see Figure 4). A likely reason is that PMF did not resolve coal combustion  
546 and biomass burning factors well as both factors presented a strong seasonal pattern with high  
547 concentrations during the winter. Another possibility is the difficulty in resolving primary and  
548 secondary fractions due to a lack of secondary organic markers used in the study. This was further  
549 supported by the fact noted above that the PMF biomass burning factor also contained some signal  
550 from coal combustion activities. The sum of coal combustion and biomass burning factors from both  
551 approaches showed a good correlation ( $r^2 = 0.7$ ,  $n = 68$ ,  $p < 0.05$ ), suggesting a common emission pattern  
552 (e.g., high in winter and low in summer), making it challenging to resolve them. Factors linked to  
553 vehicle emissions did not show any correlation. A weak correlation ( $r^2 = 0.3$ ,  $n = 68$ ,  $p < 0.05$ ) was  
554 observed between Other OC from CMB, a proxy for the secondary organic fraction and the PMF  
555 secondary inorganics factor. In addition, other OC also weakly correlated with soil dust ( $r^2 = 0.22$ ,  
556  $n = 34$ ,  $p < 0.05$ ) in summer, suggesting the mixing of unresolved secondary fraction with soil dust  
557 profile and supports the hypothesis discussed above. It should be noted that other OC could also  
558 contain unresolved primary fractions as PMF results indicated substantial influence of industrial  
559 emissions and dust related sources. However, the source profiles related to industrial emissions and  
560 dust were not accounted for in the CMB model (Xu et al., 2020).

561

562 **(b) With CMB results at PG**

563 The comparison was also made using data from both seasons at PG (Figure 5). Biomass burning  
564 aerosols showed a good correlation for both approaches ( $r^2 = 0.7$ ,  $n = 20$ ,  $p < 0.05$ ) but a substantially  
565 higher concentration was estimated by the CMB model ( $5.1 \mu\text{g m}^{-3}$  and  $2.0 \mu\text{g m}^{-3}$  by CMB and PMF  
566 respectively). A significant correlation was also seen between traffic related factors from CMB and



567 PMF (gasoline-CMB vs traffic ( $r^2=0.6$ ,  $n=20$ ,  $p<0.05$ ), diesel-CMB vs traffic ( $r^2=0.6$ ,  $n=20$ ,  $p<0.05$ )),  
568 indicating that traffic sources resolved using PMF at the PG site may have included signals from both  
569 diesel and gasoline vehicles; however it was not conclusive at the IAP site, as discussed above. This  
570 suggests the traffic source resolved using PMF may contain particles linked to traffic emissions, but  
571 the influence of other sources is prominent at IAP and resulted in poor correlation. In addition, for  
572 traffic related factors from CMB, both showed a higher concentration (gasoline-CMB= $0.8 \mu\text{g m}^{-3}$ ,  
573 diesel-CMB= $4.5 \mu\text{g m}^{-3}$ , traffic-PMF= $0.2 \mu\text{g m}^{-3}$ ). As with IAP, no significant correlation was  
574 observed between coal combustion factors from both approaches. The sum of coal combustion and  
575 biomass burning factors from both approaches also did not present a good correlation ( $r^2=0.3$ ,  $n=20$ ,  
576  $p<0.05$ ). This highlights the limitation of these methodologies to apportion sources when extreme  
577 meteorological conditions may lead to high internal mixing of sources. Unfavourable dispersion  
578 conditions have been previously observed in the Beijing region during severe haze events in winter  
579 (Wang et al., 2014). A high correlation was observed between Other OC (CMB) and secondary  
580 inorganics (PMF) ( $r^2=0.7$ ,  $n=20$ ,  $p<0.05$ ). In addition, Other OC also showed a very high correlation  
581 with the biomass burning factor resolved from PMF ( $r^2=0.9$ ,  $n=20$ ,  $p<0.05$ ). This suggests that the  
582 biomass burning factor in PMF may contain a substantial amount of aged aerosols since carbon  
583 emitted during biomass burning is in some cases oxygenated and water soluble (Lee et al., 2008a)  
584 and is subject to rapid oxidation in the atmosphere.

585

586 (c) **With online AMS PMF factors at IAP (winter)**

587 BBOC (biomass burning OC) from PMF-AMS analysis agreed well with that from PMF ( $r^2=0.7$ ,  
588  $n=27$ ,  $p<0.05$ ;  $4.0 \mu\text{g m}^{-3}$  and  $3.1 \mu\text{g m}^{-3}$  by online AMS and PMF, respectively) (Figure 6). Coal  
589 combustion related factors showed a modest correlation (CCOC (coal combustion OC) vs coal  
590 combustion-PMF,  $r^2=0.4$ ,  $n=27$ ,  $p<0.05$ ) but the mass concentration of the coal combustion source  
591 by PMF ( $11.3 \mu\text{g m}^{-3}$ ) is significantly higher than by PMF-AMS (CCOC= $4.7 \mu\text{g m}^{-3}$ ). This may  
592 partly be due to the different size cut offs used by these measurements ( $\text{PM}_1$  for AMS vs  $\text{PM}_{2.5}$ ). In



593 addition, significant improvement on the correlation was seen if two outlying points were removed  
594 ( $r^2=0.8$ , see Figure 6). Oxygenated fractions from AMS, MOOOC (more oxidised oxygenated OC)  
595 and LOOOC (low oxidised oxygenated OC) also exhibited a good correlation with secondary  
596 inorganics (LOOOC vs secondary inorganics ( $r^2=0.6$ ,  $n=27$ ,  $p<0.05$ , LOOOC= $2.9 \mu\text{g m}^{-3}$ , secondary  
597 inorganics= $1.6 \mu\text{g m}^{-3}$ ), MOOOC vs secondary inorganics ( $r^2=0.7$ ,  $n=27$ ,  $p<0.05$ , MOOOC= $4.4 \mu\text{g}$   
598  $\text{m}^{-3}$ ). This was also confirmed by LOOOC and MOOOC showing a good correlation with  $\text{NO}_3^-$  and  
599  $\text{SO}_4^{2-}$  previously (Cao et al., 2017). This suggests the oxygenated fractions from AMS and secondary  
600 inorganics are subject to similar controls in the atmosphere. In addition, both oxygenated fractions  
601 were also found to be correlated with biomass burning aerosols (LOOOC vs biomass burning-PMF  
602 ( $r^2=0.7$ ,  $n=27$ ,  $p<0.05$ ), MOOOC vs biomass burning-PMF ( $r^2=0.6$ ,  $n=27$ ,  $p<0.05$ )). This further  
603 highlights a potentially important role of biomass burning activity in SOA formation at IAP. A good  
604 correlation was also observed between OPOC (oxidised primary OC) and secondary inorganics and  
605 biomass burning ( $r^2=0.7$ ,  $n=27$ ,  $p<0.05$ ).

606

#### 607 (d) Offline AMS PMF factors at IAP (winter)

608 BBOC from PMF-offline AMS analysis showed a good correlation with that from PMF ( $r^2=0.6$ ,  $n=32$ ,  
609  $p<0.05$ ) (Figure 7) but the mass concentration of BBOC ( $4.6 \mu\text{g m}^{-3}$ ) is higher than biomass burning  
610 ( $3.1 \mu\text{g m}^{-3}$ ) from PMF. This was also noticed above while comparing with BBOC resolved using  
611 online AMS PMF, suggesting a potential uncertainty in estimating the source contribution from  
612 biomass burning. The uncertainty in filter-based PMF analysis could be related to model error. This  
613 was further supported as biomass burning factor also made significant contributions to  $\text{Ca}^{2+}$  (15%),  
614 Ni (30%), Cu (50%), and Al (35%), and these species are not necessarily from biomass burning  
615 emissions but they were not resolved by PMF. In addition, the uncertainties linked to PMF-AMS  
616 analysis could also contribute. A high correlation was noticed for secondary factors resolved using  
617 both approaches (OOC (oxygenated OC) vs Secondary inorganics,  $r^2=0.8$ ,  $n=32$ ,  $p<0.05$ ). OOC also  
618 showed a good correlation with the biomass burning factor (OOC vs biomass burning-PMF,  $r^2=0.7$ ,



619  $n=32$ ,  $p<0.05$ ). This supports the hypothesis discussed previously on the origin of oxygenated  
620 fractions.

621  
622 Overall, the comparison of filter based PMF results was in broad agreement with other receptor  
623 modelling approaches applied on the same dataset. However, large discrepancies were also observed  
624 for some factors / sources. Common sources such as biomass burning and coal combustion were well  
625 resolved using all approaches with some exceptions observed when using filter based PMF approach.  
626 This could be linked to internal mixing of sources when the influence of climate and local  
627 meteorology on both sources is predominant and making it challenging to resolve using PMF. A good  
628 agreement was also observed between secondary inorganic aerosols and secondary fractions resolved  
629 using other approaches. However, sources identified based on metal signatures using PMF indicated  
630 some mixing or mis-attribution. For example, the influence of unresolved SOC on the soil dust profile  
631 was observed during summer.

632

### 633 **3.3. Comparison with Previous PMF Source Apportionment Results in Beijing**

634 In this section an attempt has been made to understand the PM sources identified in the Beijing  
635 metropolitan area by previous studies. The goal was here to assess the previous PMF source  
636 apportionment results and report any discrepancies noticed in the resolved sources using PMF. This  
637 may provide useful insight on sources resolved in the present study and also in exploring the issues  
638 associated with filter based PMF modelling in the Beijing metropolitan area. Details of the studies  
639 conducted to evaluate PM sources using a PMF model applied to inorganic and organic markers in  
640 the Beijing metropolitan area are presented in Table 1 and the major outcomes are discussed hereafter.

641  
642 Overall, these previous PMF studies provide insights on PM sources in the Beijing metropolitan area  
643 (Li et al., 2019; Ma et al., 2017a; Tian et al., 2016; Yu et al., 2013; Song et al., 2007; Song et al.,  
644 2006; Liu et al., 2019; Wang et al., 2008; Zhang et al., 2013). The major identified sources are dust,



645 traffic emissions, coal combustion, industrial activity, secondary inorganic aerosols and biomass  
646 burning. Although there is a general issue of their inability to identify sources such as secondary  
647 organic aerosol and cooking emissions, similar to the present study, due to the lack of organic markers  
648 used in the PMF model to apportion these sources. However, beyond this, their PMF outcomes were  
649 not consistent. Large discrepancies between the sources were seen (Table 1) based on the sources  
650 identified as well as their contribution to PM mass concentrations. Several factors could cause these  
651 differences such as the chemical species used as input in the PMF model, the period of the study,  
652 identification of sources based on chemical signatures and changes to the sources with time.

653  
654 Input species considered within the previous studies were combinations of water-soluble ions,  
655 metallic elements, OC and EC. Similar input species were used in all of these studies, with the  
656 exception of the studies by Yu et al. (2013) and Li et al. (2019) who used only metallic elements for  
657 the source apportionment. As shown in this study, including organic markers may help to resolve  
658 some of the primary sources.

659

660 Another important parameter, the chemical species used for identifying sources were not always  
661 consistent. For example, coal combustion was resolved based on high contribution of OC, EC, and  
662 Cl present in the factor profile by Zhang et al. (2013), Wang et al. (2008), Song et al. (2007) and Song  
663 et al. (2006), in accordance with source profiles determined in the laboratory (Zheng et al., 2005).  
664 High Cl associated with fine aerosols in winter is a distinctive feature in Beijing and even around  
665 inland China, which is ascribed to coal combustion (Wang et al., 2008). Contrarily, Tian et al. (2016)  
666 identified coal combustion based on a high contribution of OC and EC, while the high contribution  
667 of Cl was attributed to a biomass burning source, similar to another study (Ma et al., 2017a). In other  
668 studies (Li et al., 2019; Yu et al., 2013; Liu et al., 2019) coal combustion was resolved based on the  
669 presence of metallic elements such as V, Se, Co, Cd, As and Ni, where V and Ni are widely used  
670 markers for oil combustion (Mazzei et al., 2008). High loadings of As and Se have also been reported



671 as a typical source characteristic of coal combustion (Vejahati et al., 2010). Similar to coal  
672 combustion, biomass burning was often characterised using the presence of K (Li et al., 2019; Tian  
673 et al., 2016; Yu et al., 2013; Song et al., 2007; Song et al., 2006; Zhang et al., 2013; Liu et al., 2019;  
674 Wang et al., 2008), a typical marker of biomass burning. Farming in Beijing's suburban districts has  
675 been extensive in recent years. Burning of the crop remnants and fallen leaves by farmers in autumn  
676 and winter results in the enhanced emissions of K. In addition, the contributions of Cl and Na were  
677 also considered for the identification of these sources in some cases, depending on the species used  
678 within the input (Song et al., 2007; Song et al., 2006; Tian et al., 2016). This highlights the fact that  
679 none of the studies have used organic markers such as picene and levoglucosan which are very  
680 specific to these combustion sources as discussed before, which may cause uncertainty in the resolved  
681 sources. However, in the present study the use of organic markers played a key role in the  
682 identification of these sources and their better apportionment. Despite this, some issues were observed  
683 with these identified sources during winter due to extreme meteorological conditions as well as co-  
684 emission of these aerosols at the same time, probably indicative of poor performance of the PMF  
685 model under certain conditions.

686

687 Other important sources linked to traffic emissions, industrial activities and dust, are commonly  
688 resolved among all the studies. The characterisation of these sources was predominantly based on the  
689 metallic elements. For example, Zn, Cu, and Pb including sometimes EC were most often used to  
690 characterise traffic emissions among all previous studies. Both Zn and Cu have been identified within  
691 brake linings and tyre fragments (Thorpe and Harrison, 2008) and Pb has been used in the past within  
692 gasoline as an anti-knock additive in China (Li et al., 2019). However, Cu and Zn can also serve as  
693 indicators for industrial sources (Li et al., 2017; Yu et al., 2013). Other metallic elements (e.g., Sb,  
694 Cr, Mn, K, Br and Ba) were also considered in certain cases to trace traffic emissions (Ma et al.,  
695 2017a; Tian et al., 2016; Yu et al., 2013). However, a high contribution of Cr, Mn and sometimes Fe  
696 to the given sources has also been attributed to industrial activities. Both Cr and Cr-containing



697 compounds are widely used in metallurgy, electroplating, pigment, leather and other industries  
698 (Dall'Osto et al., 2013). A previous study found that ferrous metallurgy could emit Mn (Querol et al.,  
699 2006). Furthermore, both Fe and Mn are characteristic components of iron and steel industry  
700 emissions. In addition, Co, Mg, Al, Ca, Cd, Pb, Tl, Zn, V, Ni and Cu were also considered for the  
701 apportionment of industrial sources (Tian et al., 2016; Yu et al., 2013). Zhang et al. (2013) identified  
702 a mixed source of traffic and incineration emissions, based on high loading of Cu, Zn, Cd, Pb, Sb,  
703 Sn, Mo, NO<sub>3</sub> and EC. In the present study, the assignment of road traffic emissions was based on  
704 high loadings of Zn and Pb. It was also seen that the given source may contain some influence from  
705 industrial activities, as the industrial contribution was not resolved like previous studies and probably  
706 accounted in other factors. Thus, it is clear that these metals could belong to several sources and their  
707 proper assignment to respective sources is difficult in the complex environment.

708

709 The same issue was observed with the assignments of dust type (dust/road dust/soil dust/mineral  
710 dust/yellow dust/local dust) sources. Although the dust type sources were often found to be composed  
711 of crustal elements (e.g., Ca, Mg, Si, Ti, Al, Fe), the attribution of crustal elements to a particular  
712 source was not consistent from one study to another previously. The two dust sources (road dust and  
713 soil dust) identified in the present study also indicated mixing with other factors.

714

715 The identification of the secondary inorganic aerosol factors was often based on the high contribution  
716 of water soluble ions (NO<sub>3</sub><sup>-</sup>, SO<sub>4</sub><sup>2-</sup>, NH<sub>4</sub><sup>+</sup>), consistent with other studies (Ma et al., 2017a; Song et al.,  
717 2007; Song et al., 2006; Tian et al., 2016; Liu et al., 2019; Wang et al., 2008; Zhang et al., 2013).  
718 These results highlight the role of chemical species used in characterising source profiles and their  
719 influence on the variability noticed in the Beijing metropolitan area. This issue arises because many  
720 of these species are not source specific, making it challenging to directly link PMF factors to sources.  
721 Pant and Harrison (2012), reviewing receptor modelling studies from India, noted a tendency to



722 attribute metal-rich source profiles to “industry” in a rather casual manner without evidence of local  
723 industrial sources.

724  
725 The change in sources and emissions over the course of time due to stringent emissions regulations  
726 could also be considered plausible for the observed variability in the chemical profile and contribution  
727 of identified sources. Li et al. (2019) showed levels of trace metals (V, Cr, Mn, As, Cd and Pb)  
728 decreased more than 40% due to the emission regulations, while crustal elements decreased  
729 considerably (4–45%), suggesting emissions from anthropogenic activities were suppressed. A  
730 reduction in the contribution of sources such as dust and industrial activity was observed in the present  
731 study and another recent study performed by Liu et al. (2019) relative to the previous ones, indicating  
732 the effect of regulatory measures on the contribution of identified sources to PM<sub>2.5</sub>. However, the  
733 concentration of the majority of metallic elements (K, Cr, Mn, Fe, Co, Cu, Zn, As, Ag, Cd and Pb)  
734 increased when pollution levels changed from clean days to heavily polluted days. This highlights  
735 that specific atmospheric conditions could also play a major role for the observed variability. Another  
736 factor is the time of year when these studies were conducted as some of the identified sources (e.g.,  
737 coal combustion and biomass burning) exhibit typical seasonal patterns. During a low concentration  
738 period, PMF models may have difficulty in resolving sources, leading to mixing of factors.

739  
740 Overall, the present study provides a view of existing PM<sub>2.5</sub> sources in the Beijing metropolitan area  
741 by applying the PMF model to a filter-based dataset, which included water soluble ions, metals and  
742 organic markers. Despite this, factors that were resolved based on metal signatures were not fully  
743 resolved and indicate a mixing of different sources. As a part of same campaign, also discussed above,  
744 Liu et al. (2019) used a similar approach by applying PMF on high resolution (1-hour) data, which  
745 included OC, EC, ions, and metals, and did not encounter any issue. However, previous filter based  
746 PMF studies conducted in the Beijing region that mostly included ions and metals in their input  
747 dataset often showed difficulty in the proper assignment of metals to their respective sources. Even  
748 the use of metal signatures from one to another study was not consistent. This highlights that the low



749 temporal resolution of filter data could not capture fast occurring atmospheric processes in Beijing,  
750 and may lead to a “blurring” of sources by the long averaging period. Atmospheric circulation and  
751 dynamic mechanisms play a key role in persistent haze events in Beijing during the cold period (Wu  
752 et al., 2017; Feng et al., 2014). Such events are associated with the high pollution periods and will  
753 offer opportunities for chemical and physical transformation within the aerosol that lead to  
754 contravention of the requirement of receptor models for preservation of chemical profiles between  
755 source and receptor.

756

#### 757 **4. CONCLUSION**

758 This study presents the outcomes of PMF performed on the combined dataset collected at two sites  
759 (IAP and PG) in the Beijing metropolitan area, including their comparison with source apportionment  
760 results from other approaches or based on different measurements. The PMF analysis resulted in the  
761 identification of seven sources: coal combustion, biomass burning, oil combustion, secondary  
762 inorganics, traffic emissions, road dust and soil dust. These results were in a good agreement with  
763 previously published source apportionment results made using PMF. However, factors that were  
764 resolved based on metal signatures were not fully resolved and indicate an internal mixing of different  
765 sources. In particular, soil dust, road dust and some industrial sources have many elements in common  
766 and are very difficult to distinguish.

767

768 PMF results were compared with sources resolved from CMB and with PMF performed on other  
769 measurements (online AMS, offline AMS). Results showed a broad agreement with some notable  
770 exceptions. While this study provides some confirmatory evidence on PM<sub>2.5</sub> source apportionment in  
771 Beijing, it highlights weaknesses of the PMF method when applied in this locality, and the results  
772 should be viewed in the context of studies using other methods such as CMB which appear able to  
773 give a more comprehensive view of the key sources affecting air quality. No industrial source profiles



774 were used as inputs to the CMB model reported here, so CMB offers no further insights into possible  
775 contributions from industry.

776

777 **AUTHOR CONTRIBUTIONS**

778 This study was conceived by ZS and RMH. DS performed the PMF analysis and wrote the paper with  
779 the help of Z.S. and R.M.H. T.V.V. and D.L. conducted the aerosol sampling and laboratory-based  
780 chemical analyses. X.W. and J.X. conducted the CMB modelling at PG and IAP sites, respectively.

781 All authors discussed the paper and approved the final version for publication.

782

783 **COMPETING INTERESTS**

784 The authors declare that they have no conflict of interest.

785

786 **SPECIAL ISSUE STATEMENT**

787 This article is part of the special issue “In-depth study of air pollution sources and processes within  
788 Beijing and its surrounding region (APHH-Beijing) (ACP/AMT inter-journal SI)”. It is not associated  
789 with a conference.

790

791 **FINANCIAL SUPPORT**

792 This research has been supported by the Natural Environment Research Council (APHH and SOA  
793 grants): NE/N007190/1 (AIRPOLL-Beijing), NE/S006699/1 (SOA).

794



795 **REFERENCES**

- 796 Amato, F., Pandolfi, M., Escrig, A., Querol, X., Alastuey, A., Pey, J., Perez, N., and Hopke, P. K.:  
797 Quantifying road dust resuspension in urban environment by Multilinear Engine: A comparison with  
798 PMF2, *Atmos. Environ.*, 43, 2770-2780, <https://doi.org/10.1016/j.atmosenv.2009.02.039>, 2009.  
799
- 800 Amato, F., and Hopke, P. K.: Source apportionment of the ambient PM<sub>2.5</sub> across St. Louis using  
801 constrained positive matrix factorization, *Atmos. Environ.*, 46, 329-337,  
802 <https://doi.org/10.1016/j.atmosenv.2011.09.062>, 2012.  
803
- 804 Batterman, S., Xu, L., Chen, F., Chen, F., and Zhong, X.: Characteristics of PM<sub>(2.5)</sub> Concentrations  
805 across Beijing during 2013-2015, *Atmos. Environ.* (Oxford, England: 1994), 145, 104-114,  
806 [10.1016/j.atmosenv.2016.08.060](https://doi.org/10.1016/j.atmosenv.2016.08.060), 2016.  
807
- 808 Bi, X., Simoneit, B. R. T., Sheng, G., and Fu, J.: Characterization of molecular markers in smoke  
809 from residential coal combustion in China, *Fuel*, 87, 112-119,  
810 <https://doi.org/10.1016/j.fuel.2007.03.047>, 2008.  
811
- 812 Boucher, O., Randall, D., Artaxo, P., Bretherton, C., Feingold, G., Forster, P., Kerminen, V.-M.,  
813 Kondo, Y., Liao, H., and Lohmann, U.: Clouds and aerosols, in: *Climate change 2013: the physical  
814 science basis. Contribution of Working Group I to the Fifth Assessment Report of the  
815 Intergovernmental Panel on Climate Change*, Cambridge University Press, 571-657, 2013.  
816
- 817 Cai, T., Zhang, Y., Fang, D., Shang, J., Zhang, Y., and Zhang, Y.: Chinese vehicle emissions  
818 characteristic testing with small sample size: Results and comparison, *Atmospheric Pollution  
819 Research*, 8, 154-163, <https://doi.org/10.1016/j.apr.2016.08.007>, 2017.  
820
- 821 Canepari, S., Perrino, C., Olivieri, F., and Astolfi, M. L.: Characterisation of the traffic sources of  
822 PM through size-segregated sampling, sequential leaching and ICP analysis, *Atmos. Environ.*, 42,  
823 8161-8175, <https://doi.org/10.1016/j.atmosenv.2008.07.052>, 2008.  
824
- 825 Cao, L., Zhu, Q., Huang, X., Deng, J., Chen, J., Hong, Y., Xu, L., and He, L.: Chemical  
826 characterization and source apportionment of atmospheric submicron particles on the western coast  
827 of Taiwan Strait, China, *J. Environ. Sci.*, 52, 293-304, <https://doi.org/10.1016/j.jes.2016.09.018>,  
828 2017.  
829
- 830 Chan, Y., Simpson, R., McTainsh, G., Vowles, P., Cohen, D., and Bailey, G. J. A. E.: Characterisation  
831 of chemical species in PM<sub>2.5</sub> and PM<sub>10</sub> aerosols in Brisbane, Australia, *Atmos. Environ.*, 31, 3773-  
832 3785, 1997.  
833
- 834 Dall'Osto, M., Querol, X., Amato, F., Karanasiou, A., Lucarelli, F., Nava, S., Calzolari, G., and Chiari,  
835 M.: Hourly elemental concentrations in PM<sub>2.5</sub> aerosols sampled simultaneously at urban background  
836 and road site during SAPUSS - diurnal variations and PMF receptor modelling, *Atmos. Chem. Phys.*,  
837 13, 4375, 2013.  
838
- 839 Draxler, R.: *Hysplit4 User's Guide*. NOAA Tech. Memo. ERL ARL-230, 35 pp.  
840 [http://www.arl.noaa.gov/documents/reports/hysplit\\_user\\_guide.pdf](http://www.arl.noaa.gov/documents/reports/hysplit_user_guide.pdf), 1999.  
841
- 842 Duong, T. T. T., and Lee, B.-K.: Determining contamination level of heavy metals in road dust from  
843 busy traffic areas with different characteristics, *J. Environ. Manage.*, 92, 554-562,  
844 <https://doi.org/10.1016/j.jenvman.2010.09.010>, 2011.  
845



- 846 Duvall, R. M., Majestic, B. J., Shafer, M. M., Chuang, P. Y., Simoneit, B. R. T., and Schauer, J. J.:  
847 The water-soluble fraction of carbon, sulfur, and crustal elements in Asian aerosols and Asian soils,  
848 *Atmos. Environ.*, 42, 5872-5884, <https://doi.org/10.1016/j.atmosenv.2008.03.028>, 2008.
- 849  
850 Eglinton, G., Gonzalez, A. G., Hamilton, R. J., and Raphael, R. A.: Hydrocarbon constituents of the  
851 wax coatings of plant leaves: A taxonomic survey, *Phytochemistry*, 1, 89-102,  
852 [https://doi.org/10.1016/S0031-9422\(00\)88006-1](https://doi.org/10.1016/S0031-9422(00)88006-1), 1962.
- 853  
854 Feng, X., Li, Q., Zhu, Y., Wang, J., Liang, H., and Xu, R.: Formation and dominant factors of haze  
855 pollution over Beijing and its peripheral areas in winter, *Atmos. Pollut. Res.*, 5, 528-538,  
856 <https://doi.org/10.5094/APR.2014.062>, 2014.
- 857  
858 GBD MAPS Working Group: Burden of Disease Attributable to Coal-Burning and Other Major  
859 Sources of Air Pollution in China, Special Report 20, Health Effects Institute, Boston, MA, 2016.
- 860  
861 Grigoratos, T., and Martini, G.: Brake wear particle emissions: a review, *Environ. Sci. Pollut. Res.*,  
862 22, 2491-2504, 10.1007/s11356-014-3696-8, 2015.
- 863  
864 Gu, Y., Huang, R.-J., Li, Y., Duan, J., Chen, Q., Hu, W., Zheng, Y., Lin, C., Ni, H., Dai, W., Cao, J.,  
865 Liu, Q., Chen, Y., Chen, C., Ovadnevaite, J., Ceburnis, D., and O'Dowd, C.: Chemical nature and  
866 sources of fine particles in urban Beijing: Seasonality and formation mechanisms, *Environ. Intl*, 140,  
867 105732, <https://doi.org/10.1016/j.envint.2020.105732>, 2020.
- 868  
869 Guo, H., Zhou, J., Wang, L., Zhou, Y., Yuan, J., and Zhao, R.: Seasonal variations and sources of  
870 carboxylic acids in PM<sub>2.5</sub> in Wuhan, China, *Aerosol Air. Qual. Res.*, 15, 517-528,  
871 10.4209/aaqr.2014.02.0040, 2015.
- 872  
873 Harrison, R. M., Vu, T. V., Jafar, H., and Shi, Z.: More mileage in reducing urban air pollution from  
874 road traffic, *Environ. Int.*, 149, 106329, <https://doi.org/10.1016/j.envint.2020.106329>, 2021.
- 875  
876 He, G., Pan, Y., and Tanaka, T.: The short-term impacts of COVID-19 lockdown on urban air  
877 pollution in China, *Nature Sustainability*, 3, 1005-1011, 10.1038/s41893-020-0581-y, 2020.
- 878  
879 Heal, M. R., Kumar, P., and Harrison, R. M.: Particles, air quality, policy and health, *Chem. Soc.*  
880 *Rev.*, 41, 6606-6630, 2012.
- 881  
882 Henry, R., Norris, G. A., Vedantham, R., and Turner, J. R.: Source Region Identification Using  
883 Kernel Smoothing, *Environ. Sci. Technol.*, 43, 4090-4097, 10.1021/es8011723, 2009.
- 884  
885 Herrera Murillo, J., Campos Ramos, A., Ángeles García, F., Blanco Jiménez, S., Cárdenas, B., and  
886 Mizohata, A.: Chemical composition of PM<sub>2.5</sub> particles in Salamanca, Guanajuato Mexico: Source  
887 apportionment with receptor models, *Atmos. Res.*, 107, 31-41, 10.1016/j.atmosres.2011.12.010,  
888 2012.
- 889  
890 Hopke, P. K.: Review of receptor modeling methods for source apportionment, *JAWMA*, 66, 237-  
891 259, 10.1080/10962247.2016.1140693, 2016.
- 892  
893 Hu, W., Hu, M., Hu, W., Jimenez, J. L., Yuan, B., Chen, W., Wang, M., Wu, Y., Chen, C., Wang, Z.,  
894 Peng, J., Zeng, L., and Shao, M.: Chemical composition, sources, and aging process of submicron  
895 aerosols in Beijing: Contrast between summer and winter, 121, 1955-1977, 10.1002/2015jd024020,  
896 2016.
- 897



- 898 Huang, X., Tang, G., Zhang, J., Liu, B., Liu, C., Zhang, J., Cong, L., Cheng, M., Yan, G., Gao, W.,  
899 Wang, Y., and Wang, Y.: Characteristics of PM<sub>2.5</sub> pollution in Beijing after the improvement of air  
900 quality, *J. Environ. Sci.*, 100, 1-10, <https://doi.org/10.1016/j.jes.2020.06.004>, 2021.  
901
- 902 Huang, X. F., He, L. Y., Hu, M., Canagaratna, M. R., Sun, Y., Zhang, Q., Zhu, T., Xue, L., Zeng, L.  
903 W., Liu, X. G., Zhang, Y. H., Jayne, J. T., Ng, N. L., and Worsnop, D. R.: Highly time-resolved  
904 chemical characterization of atmospheric submicron particles during 2008 Beijing Olympic Games  
905 using an Aerodyne High-Resolution Aerosol Mass Spectrometer, *Atmos. Chem. Phys.*, 10, 8933-  
906 8945, 10.5194/acp-10-8933-2010, 2010a.  
907
- 908 Huang, X. F., He, L. Y., Hu, M., Canagaratna, M. R., Sun, Y., Zhang, Q., Zhu, T., Xue, L., Zeng, L.  
909 W., Liu, X. G., Zhang, Y. H., Jayne, J. T., Ng, N. L., and Worsnop, D. R.: Highly time-resolved  
910 chemical characterization of atmospheric submicron particles during 2008 Beijing Olympic Games  
911 using an Aerodyne High-Resolution Aerosol Mass Spectrometer, *Atmos. Chem. Phys.*, 10, 8933-  
912 8945, 10.5194/acp-10-8933-2010, 2010b.  
913
- 914 Jaekels, J. M., Bae, M.-S., and Schauer, J. J.: Positive matrix factorization (PMF) analysis of  
915 molecular marker measurements to quantify the sources of organic aerosols, *Environ. Sci. Technol.*,  
916 41, 5763-5769, 2007.  
917
- 918 Ji, D., Li, L., Wang, Y., Zhang, J., Cheng, M., Sun, Y., Liu, Z., Wang, L., Tang, G., and Hu, B. J. A.  
919 E.: The heaviest particulate air-pollution episodes occurred in northern China in January, 2013:  
920 Insights gained from observation, *Atmos. Environ.*, 92, 546-556,  
921 [doi.org/10.1016/j.atmosenv.2014.04.048](https://doi.org/10.1016/j.atmosenv.2014.04.048), 2014.  
922
- 923 Jing, B., Wu, L., Mao, H., Gong, S., He, J., Zou, C., Song, G., Li, X., and Wu, Z.: Development of a  
924 vehicle emission inventory with high temporal-spatial resolution based on NRT traffic data and its  
925 impact on air pollution in Beijing – Part 1: Development and evaluation of vehicle emission  
926 inventory, *Atmos. Chem. Phys.*, 16, 3161-3170, 10.5194/acp-16-3161-2016, 2016.  
927
- 928 Kim, E.-A., and Koh, B.: Utilization of road dust chemical profiles for source identification and  
929 human health impact assessment, *Sci. Rep.*, 10, 14259, 10.1038/s41598-020-71180-x, 2020.  
930
- 931 Kolattukudy, P. E.: *Chemistry and biochemistry of natural waxes*, Elsevier Scientific Pub. Co., 1976.  
932
- 933 Laing, J. R., Hopke, P. K., Hopke, E. F., Husain, L., Dutkiewicz, V. A., Paatero, J., and Viisanen, Y.:  
934 Positive Matrix Factorization of 47 Years of Particle Measurements in Finnish Arctic, *Aerosol. Air*  
935 *Qual. Res.*, 15, 188-207 2015.  
936
- 937 Le, T., Wang, Y., Liu, L., Yang, J., Yung, Y. L., Li, G., and Seinfeld, J. H.: Unexpected air pollution  
938 with marked emission reductions during the COVID-19 outbreak in China, *Science*, 369, 702,  
939 [10.1126/science.abb7431](https://doi.org/10.1126/science.abb7431), 2020.  
940
- 941 Lee, B.-K., Hieu, N. T. J. A., and Resarch, A. Q.: Seasonal variation and sources of heavy metals in  
942 atmospheric aerosols in a residential area of Ulsan, Korea, 11, 679-688, 2011.  
943
- 944 Lee, S., Kim, H. K., Yan, B., Cobb, C. E., Hennigan, C., Nichols, S., Chamber, M., Edgerton, E. S.,  
945 Jansen, J. J., Hu, Y., Zheng, M., Weber, R. J., and Russell, A. G.: Diagnosis of Aged Prescribed  
946 Burning Plumes Impacting an Urban Area, *Environ. Sci. Technol.*, 42, 1438-1444,  
947 [10.1021/es7023059](https://doi.org/10.1021/es7023059), 2008a.



- 948 Lee, S., Liu, W., Wang, Y., Russell, A. G., and Edgerton, E. S.: Source apportionment of PM 2.5:  
949 Comparing PMF and CMB results for four ambient monitoring sites in the southeastern United States,  
950 Atmos. Environ., 42, 4126-4137, 2008b.  
951
- 952 Li, M., Liu, Z., Chen, J., Huang, X., Liu, J., Xie, Y., Hu, B., Xu, Z., Zhang, Y., and Wang, Y.:  
953 Characteristics and source apportionment of metallic elements in PM<sub>2.5</sub> at urban and suburban sites  
954 in Beijing: Implication of emission reduction, 10, 105, 2019.  
955
- 956 Li, D., Liu, J., Zhang, J., Gui, H., Du, P., Yu, T., Wang, J., Lu, Y., Liu, W., and Cheng, Y.:  
957 Identification of long-range transport pathways and potential sources of PM(2.5) and PM(10) in  
958 Beijing from 2014 to 2015, J. Environ. Sci. (China), 56, 214-229, 10.1016/j.jes.2016.06.035, 2017.  
959
- 960 Lim, J.-M., Lee, J.-H., Moon, J.-H., Chung, Y.-S., and Kim, K.-H.: Source apportionment of PM<sub>10</sub> at  
961 a small industrial area using Positive Matrix Factorization, Atmos. Res., 95, 88-100,  
962 <https://doi.org/10.1016/j.atmosres.2009.08.009>, 2010.  
963
- 964 Liu, Y., Zheng, M., Yu, M., Cai, X., Du, H., Li, J., Zhou, T., Yan, C., Wang, X., Shi, Z., Harrison, R.  
965 M., Zhang, Q., and He, K.: High-time-resolution source apportionment of PM<sub>2.5</sub> in Beijing with  
966 multiple models, Atmos. Chem. Phys., 19, 6595-6609, 10.5194/acp-19-6595-2019, 2019.  
967
- 968 Lu, X., Yuan, D., Chen, Y., and Fung, J. C. H.: Impacts of urbanization and long-term meteorological  
969 variations on global PM<sub>2.5</sub> and its associated health burden, Environ. Pollut., 270, 116003,  
970 <https://doi.org/10.1016/j.envpol.2020.116003>, 2021.  
971
- 972 Ma, Q., Wu, Y., Tao, J., Xia, Y., Liu, X., Zhang, D., Han, Z., Zhang, X., and Zhang, R.: Variations  
973 of Chemical composition and source apportionment of PM<sub>2.5</sub> during winter haze episodes in Beijing,  
974 Aerosol. Air Qual. Res., 17, 2791-2803, 10.4209/aaqr.2017.10.0366, 2017a.  
975
- 976 Ma, Q., Wu, Y., Zhang, D., Wang, X., Xia, Y., Liu, X., Tian, P., Han, Z., Xia, X., Wang, Y., and  
977 Zhang, R.: Roles of regional transport and heterogeneous reactions in the PM<sub>2.5</sub> increase during winter  
978 haze episodes in Beijing, Sci. Tot. Environ., 599-600, 246-253,  
979 <https://doi.org/10.1016/j.scitotenv.2017.04.193>, 2017b.  
980
- 981 Mazzei, F., D'Alessandro, A., Lucarelli, F., Nava, S., Prati, P., Valli, G., and Vecchi, R.:  
982 Characterization of particulate matter sources in an urban environment, Sci. Tot. Environ., 401, 81-  
983 89, <https://doi.org/10.1016/j.scitotenv.2008.03.008>, 2008.  
984
- 985 Niu, H., Hu, W., Zhang, D., Wu, Z., Guo, S., Pian, W., Cheng, W., and Hu, M.: Variations of fine  
986 particle physiochemical properties during a heavy haze episode in the winter of Beijing, Sci. Tot.  
987 Environ., 571, 103-109, <https://doi.org/10.1016/j.scitotenv.2016.07.147>, 2016.  
988
- 989 Norris, G., Duvall, R., Brown, S., and Bai, S.: EPA Positive Matrix Factorization (PMF) 5.0  
990 fundamentals and User Guide Prepared for the US Environmental Protection Agency Office of  
991 Research and Development, Washington, DC, DC EPA/600/R-14/108, 2014.  
992
- 993 Oros, D. R., and Simoneit, B. R. T.: Identification and emission rates of molecular tracers in coal  
994 smoke particulate matter, Fuel, 79, 515-536, [https://doi.org/10.1016/S0016-2361\(99\)00153-2](https://doi.org/10.1016/S0016-2361(99)00153-2), 2000.  
995
- 996 Paatero, P., and Hopke, P. K.: Discarding or downweighting high-noise variables in factor analytic  
997 models, Anal. Chim. Acta, 490, 277-289, 2003.  
998



- 999 Paatero, P.: Least squares formulation of robust non-negative factor analysis, *Chemom. Intell. Lab.*  
1000 *Syst.*, 37, 23-35, [https://doi.org/10.1016/S0169-7439\(96\)00044-5](https://doi.org/10.1016/S0169-7439(96)00044-5), 1997.
- 1001
- 1002 Paatero, P., and Tapper, U.: Positive matrix factorization: A non-negative factor model with optimal  
1003 utilization of error estimates of data values, *Environmetrics*, 5, 111-126, 1994.
- 1004
- 1005 Pacyna, J. M., and Pacyna, E. G.: An assessment of global and regional emissions of trace metals to  
1006 the atmosphere from anthropogenic sources worldwide, *Environ. Rev.*, 9, 269-298, 10.1139/a01-012,  
1007 2001.
- 1008
- 1009 Pant, P., Shukla, A., Kohl, S. D., Chow, J. C., Watson, J. G., and Harrison, R. M.: Characterization  
1010 of ambient PM<sub>2.5</sub> at a pollution hotspot in New Delhi, India and inference of sources, *Atmos.*  
1011 *Environ.*, 109, 178-189, <http://dx.doi.org/10.1016/j.atmosenv.2015.02.074>, 2015.
- 1012
- 1013 Pant, P., and Harrison, R. M.: Estimation of the contribution of road traffic emissions to particulate  
1014 matter concentrations from field measurements: A review, *Atmos. Environ.*, 77, 78-97,  
1015 <https://doi.org/10.1016/j.atmosenv.2013.04.028>, 2013.
- 1016
- 1017 Pant, P., and Harrison, R. M.: Critical review of receptor modelling for particulate matter: a case  
1018 study of India, *Atmos. Environ.*, 49, 1-12, 2012.
- 1019
- 1020 Paraskevopoulou, D., Liakakou, E., Gerasopoulos, E., Theodosi, C., and Mihalopoulos, N.: Long-  
1021 term characterization of organic and elemental carbon in the PM<sub>2.5</sub> fraction: the case of Athens,  
1022 Greece, *Atmos. Chem. Phys.*, 14, 13313-13325, 10.5194/acp-14-13313-2014, 2014.
- 1023
- 1024 Paulot, F., Paynter, D., Ginoux, P., Naik, V., Whitburn, S., Van Damme, M., Clarisse, L., Coheur, P.-  
1025 F., and Horowitz, L. W.: Gas-aerosol partitioning of ammonia in biomass burning plumes:  
1026 Implications for the interpretation of spaceborne observations of ammonia and the radiative forcing  
1027 of ammonium nitrate, 44, 8084-8093, <https://doi.org/10.1002/2017GL074215>, 2017.
- 1028
- 1029 Petit, J. E., Favez, O., Albinet, A., and Canonaco, F.: A user-friendly tool for comprehensive  
1030 evaluation of the geographical origins of atmospheric pollution: Wind and trajectory analyses,  
1031 *Environ. Modell. Softw.*, 88, 183-187, <https://doi.org/10.1016/j.envsoft.2016.11.022>, 2017.
- 1032
- 1033 Piscitello, A., Bianco, C., Casasso, A., and Sethi, R.: Non-exhaust traffic emissions: Sources,  
1034 characterization, and mitigation measures, *Sci. Total Environ.*, 766, 144440,  
1035 <https://doi.org/10.1016/j.scitotenv.2020.144440>, 2021.
- 1036
- 1037 Polissar, A. V., Hopke, P. K., and Poirot, R. L.: Atmospheric aerosol over Vermont: chemical  
1038 composition and sources, *Environ. Sci. Technol.*, 35, 4604-4621, 2001.
- 1039
- 1040 Polissar, A. V., Hopke, P. K., Paatero, P., Malm, W. C., and Sisler, J. F.: Atmospheric aerosol over  
1041 Alaska: 2. Elemental composition and sources, *J. Geophys. Res.-Atmos.*, 103, 19045-19057, 1998.
- 1042
- 1043 Qiu, Y., Xie, Q., Wang, J., Xu, W., Li, L., Wang, Q., Zhao, J., Chen, Y., Chen, Y., Wu, Y., Du, W.,  
1044 Zhou, W., Lee, J., Zhao, C., Ge, X., Fu, P., Wang, Z., Worsnop, D. R., and Sun, Y.: Vertical  
1045 Characterization and Source Apportionment of Water-Soluble Organic Aerosol with High-resolution  
1046 Aerosol Mass Spectrometry in Beijing, China, *ACS Earth Space Chem.*, 3, 273-284,  
1047 10.1021/acsearthspacechem.8b00155, 2019.



- 1048 Querol, X., Zhuang, X., Alastuey, A., Viana, M., Lv, W., Wang, Y., López, A., Zhu, Z., Wei, H., and  
1049 Xu, S.: Speciation and sources of atmospheric aerosols in a highly industrialised emerging mega-city  
1050 in Central China, *J. Environ. Monit.*, 8, 1049-1059, 10.1039/B608768J, 2006.
- 1051  
1052 Rogge, W. F., Hildemann, L. M., Mazurek, M. A., Cass, G. R., and Simoneit, B. R. T.: Sources of  
1053 fine organic aerosol. 4. Particulate abrasion products from leaf surfaces of urban plants, *Environ. Sci.*  
1054 *Technol.*, 27, 2700-2711, 10.1021/es00049a008, 1993.
- 1055  
1056 Schembari, C., Bove, M. C., Cuccia, E., Cavalli, F., Hjorth, J., Massabò, D., Nava, S., Udisti, R., and  
1057 Prati, P.: Source apportionment of PM<sub>10</sub> in the Western Mediterranean based on observations from a  
1058 cruise ship, *Atmos. Environ.*, 98, 510-518, 10.1016/j.atmosenv.2014.09.015, 2014.
- 1059  
1060 Shi, Z., Song, C., Liu, B., Lu, G., Xu, J., Van Vu, T., Elliott, R. J. R., Li, W., Bloss, W. J., and  
1061 Harrison, R. M.: Abrupt but smaller than expected changes in surface air quality attributable to  
1062 COVID-19 lockdowns, *Sci. Adv.*, 7, 10.1126/sciadv.abd6696, 2021.
- 1063  
1064 Shi, Z., Vu, T., Kotthaus, S., Harrison, R. M., Grimmond, S., Yue, S., Zhu, T., Lee, J., Han, Y.,  
1065 Demuzere, M., Dunmore, R. E., Ren, L., Liu, D., Wang, Y., Wild, O., Allan, J., Acton, W. J., Barlow,  
1066 J., Barratt, B., Beddows, D., Bloss, W. J., Calzolari, G., Carruthers, D., Carslaw, D. C., Chan, Q.,  
1067 Chatzidiakou, L., Chen, Y., Crilley, L., Coe, H., Dai, T., Doherty, R., Duan, F., Fu, P., Ge, B., Ge,  
1068 M., Guan, D., Hamilton, J. F., He, K., Heal, M., Heard, D., Hewitt, C. N., Hollaway, M., Hu, M., Ji,  
1069 D., Jiang, X., Jones, R., Kalberer, M., Kelly, F. J., Kramer, L., Langford, B., Lin, C., Lewis, A. C.,  
1070 Li, J., Li, W., Liu, H., Liu, J., Loh, M., Lu, K., Lucarelli, F., Mann, G., McFiggans, G., Miller, M. R.,  
1071 Mills, G., Monk, P., Nemitz, E., O'Connor, F., Ouyang, B., Palmer, P. I., Percival, C., Popoola, O.,  
1072 Reeves, C., Rickard, A. R., Shao, L., Shi, G., Spracklen, D., Stevenson, D., Sun, Y., Sun, Z., Tao, S.,  
1073 Tong, S., Wang, Q., Wang, W., Wang, X., Wang, X., Wang, Z., Wei, L., Whalley, L., Wu, X., Wu,  
1074 Z., Xie, P., Yang, F., Zhang, Q., Zhang, Y., Zhang, Y., and Zheng, M.: Introduction to the special  
1075 issue "In-depth study of air pollution sources and processes within Beijing and its surrounding region  
1076 (APHH-Beijing)", *Atmos. Chem. Phys.*, 19, 7519-7546, 10.5194/acp-19-7519-2019, 2019.
- 1077  
1078 Shrivastava, M. K., Subramanian, R., Rogge, W. F., and Robinson, A. L.: Sources of organic aerosol:  
1079 Positive matrix factorization of molecular marker data and comparison of results from different  
1080 source apportionment models, *Atmos. Environ.*, 41, 9353-9369, 10.1016/j.atmosenv.2007.09.016,  
1081 2007.
- 1082  
1083 Simoneit, B. R.: A review of biomarker compounds as source indicators and tracers for air pollution,  
1084 *Environ. Sci. Pollut. Res.*, 6, 159-169, 1999.
- 1085  
1086 Smichowski, P., Gómez, D., Frazzoli, C., and Caroli, S.: Traffic-Related Elements in Airborne  
1087 Particulate Matter, *Applied Spectroscopy Reviews*, 43, 23-49, 10.1080/05704920701645886, 2007.
- 1088  
1089 Song, Y., Tang, X., Xie, S., Zhang, Y., Wei, Y., Zhang, M., Zeng, L., and Lu, S.: Source  
1090 apportionment of PM<sub>2.5</sub> in Beijing in 2004, *J. Hazard. Mater.*, 146, 124-130,  
1091 <https://doi.org/10.1016/j.jhazmat.2006.11.058>, 2007.
- 1092  
1093 Song, Y., Zhang, Y., Xie, S., Zeng, L., Zheng, M., Salmon, L. G., Shao, M., and Slanina, S.: Source  
1094 apportionment of PM<sub>2.5</sub> in Beijing by positive matrix factorization, *Atmos. Environ.*, 40, 1526-1537,  
1095 10.1016/j.atmosenv.2005.10.039, 2006.
- 1096  
1097 Sörme, L., Bergbäck, B., and Lohm, U.: Goods in the Anthroposphere as a Metal Emission Source A  
1098 Case Study of Stockholm, Sweden, *Water, Air & Soil Pollut.: Focus*, 1, 213-227,  
1099 10.1023/A:1017516523915, 2001.



- 1100  
1101 Srimuruganandam, B., and Shiva Nagendra, S. M.: Application of positive matrix factorization in  
1102 characterization of PM<sub>10</sub> and PM<sub>2.5</sub> emission sources at urban roadside, *Chemosphere*, 88, 120-130,  
1103 <http://doi.org/10.1016/j.chemosphere.2012.02.083>, 2012.
- 1104  
1105 Srivastava, D., Tomaz, S., Favez, O., Lanzafame, G. M., Golly, B., Besombes, J. L., Alleman, L. Y.,  
1106 Jaffrezo, J. L., Jacob, V., Perraudin, E., Villenave, E., and Albinet, A.: Speciation of organic fraction  
1107 does matter for source apportionment. Part I: A one-year campaign in Grenoble (France), *Sci. Tot.*  
1108 *Environ.*, 624, 1598-1611, 10.1016/j.scitotenv.2017.12.135, 2018.
- 1109  
1110 Stein, A. F., Draxler, R. R., Rolph, G. D., Stunder, B. J. B., Cohen, M. D., and Ngan, F.: NOAA's  
1111 HYSPLIT Atmospheric Transport and Dispersion Modeling System, *Bull. Am. Meteorol. Soc.*, 96,  
1112 2059-2077, 10.1175/bams-d-14-00110.1, 2015.
- 1113  
1114 Sun, J., Zhang, Q., Canagaratna, M. R., Zhang, Y., Ng, N. L., Sun, Y., Jayne, J. T., Zhang, X., Zhang,  
1115 X., and Worsnop, D. R.: Highly time- and size-resolved characterization of submicron aerosol  
1116 particles in Beijing using an Aerodyne Aerosol Mass Spectrometer, *Atmos. Environ.*, 44, 131-140,  
1117 <https://doi.org/10.1016/j.atmosenv.2009.03.020>, 2010.
- 1118  
1119 Sun, Y., He, Y., Kuang, Y., Xu, W., Song, S., Ma, N., Tao, J., Cheng, P., Wu, C., Su, H., Cheng, Y.,  
1120 Xie, C., Chen, C., Lei, L., Qiu, Y., Fu, P., Croteau, P., and Worsnop, D. R.: Chemical differences  
1121 between PM<sub>1</sub> and PM<sub>2.5</sub> in Highly polluted environment and implications in air pollution studies,  
1122 *Geophys. Res. Lett.*, 47, e2019GL086288, 10.1029/2019GL086288, 2020.
- 1123  
1124 Sun, Y., Du, W., Fu, P., Wang, Q., Li, J., Ge, X., Zhang, Q., Zhu, C., Ren, L., Xu, W., Zhao, J., Han,  
1125 T., Worsnop, D. R., and Wang, Z.: Primary and secondary aerosols in Beijing in winter: sources,  
1126 variations and processes, *Atmos. Chem. Phys.*, 16, 8309-8329, 10.5194/acp-16-8309-2016, 2016.
- 1127  
1128 Sun, Y., Jiang, Q., Wang, Z., Fu, P., Li, J., Yang, T., and Yin, Y.: Investigation of the sources and  
1129 evolution processes of severe haze pollution in Beijing in January 2013, 119, 4380-4398,  
1130 <https://doi.org/10.1002/2014JD021641>, 2014.
- 1131  
1132 Sun, Y. L., Wang, Z. F., Fu, P. Q., Yang, T., Jiang, Q., Dong, H. B., Li, J., and Jia, J. J.: Aerosol  
1133 composition, sources and processes during wintertime in Beijing, China, *Atmos. Chem. Phys.*, 13,  
1134 4577-4592, 10.5194/acp-13-4577-2013, 2013.
- 1135  
1136 Sun, J., Zhang, Q., Canagaratna, M. R., Zhang, Y., Ng, N. L., Sun, Y., Jayne, J. T., Zhang, X., Zhang,  
1137 X., and Worsnop, D. R.: Highly time- and size-resolved characterization of submicron aerosol  
1138 particles in Beijing using an Aerodyne Aerosol Mass Spectrometer, *Atmos. Environ.*, 44, 131-140,  
1139 <https://doi.org/10.1016/j.atmosenv.2009.03.020>, 2010.
- 1140  
1141 Sun, Y., Zhuang, G., Tang, A., Wang, Y., and An, Z.: Chemical Characteristics of PM<sub>2.5</sub> and PM<sub>10</sub>  
1142 in Haze-Fog Episodes in Beijing, *Environ. Sci. Technol.*, 40, 3148-3155, 10.1021/es051533g, 2006.
- 1143  
1144 Sun, Y., Zhuang, G., Wang, Y., Zhao, X., Li, J., Wang, Z., and An, Z.: Chemical composition of dust  
1145 storms in Beijing and implications for the mixing of mineral aerosol with pollution aerosol on the  
1146 pathway, *J. Geophys. Chem.*, 110, D24209, 10.1029/2005jd006054, 2005.
- 1147  
1148 Swietlicki, E., and Krejci, R.: Source characterisation of the Central European atmospheric aerosol  
1149 using multivariate statistical methods, *Nucl. Instrum. Methods Phys. Res., Sect. B*, 109-110, 519-525,  
1150 [https://doi.org/10.1016/0168-583X\(95\)01220-6](https://doi.org/10.1016/0168-583X(95)01220-6), 1996.
- 1151



- 1152 Tao, S., Ru, M. Y., Du, W., Zhu, X., Zhong, Q. R., Li, B. G., Shen, G. F., Pan, X. L., Meng, W. J.,  
1153 Chen, Y. L., Shen, H. Z., Lin, N., Su, S., Zhuo, S. J., Huang, T. B., Xu, Y., Yun, X., Liu, J. F., Wang,  
1154 X. L., Liu, W. X., Chen, H. F., and Zhu, D. Q.: Quantifying the Rural Residential Energy Transition  
1155 in China from 1992 to 2012 through a Representative National Survey, *Nat. Energy*, 3, 567–573,  
1156 2018.
- 1157
- 1158 Thorpe, A., and Harrison, R. M.: Sources and properties of non-exhaust particulate matter from road  
1159 traffic: A review, *Sci. Tot. Environ.*, 400, 270–282, <https://doi.org/10.1016/j.scitotenv.2008.06.007>,  
1160 2008.
- 1161
- 1162 Tian, S. L., Pan, Y. P., and Wang, Y. S.: Size-resolved source apportionment of particulate matter in  
1163 urban Beijing during haze and non-haze episodes, *Atmos. Chem. Phys.*, 16, 1–19, 10.5194/acp-16-1-  
1164 2016, 2016.
- 1165
- 1166 Tie, X., Huang, R.-J., Cao, J., Zhang, Q., Cheng, Y., Su, H., Chang, D., Pöschl, U., Hoffmann, T.,  
1167 Dusek, U., Li, G., Worsnop, D. R., and O'Dowd, C. D.: Severe Pollution in China Amplified by  
1168 Atmospheric Moisture, *Sci. Rep.*, 7, 15760–15760, 10.1038/s41598-017-15909-1, 2017.
- 1169
- 1170 Vejahati, F., Xu, Z., and Gupta, R.: Trace elements in coal: Associations with coal and minerals and  
1171 their behavior during coal utilization – A review, *Fuel*, 89, 904–911,  
1172 <https://doi.org/10.1016/j.fuel.2009.06.013>, 2010.
- 1173
- 1174 Viana, M., Kuhlbusch, T. A. J., Querol, X., Alastuey, A., Harrison, R. M., Hopke, P. K., Winiwarter,  
1175 W., Vallius, M., Szidat, S., Prévôt, A. S. H., Hueglin, C., Bloemen, H., Wählin, P., Vecchi, R.,  
1176 Miranda, A. I., Kasper-Giebl, A., Maenhaut, W., and Hitzenberger, R.: Source apportionment of  
1177 particulate matter in Europe: A review of methods and results, *J. Aerosol Sci.*, 39, 827–849,  
1178 <http://dx.doi.org/10.1016/j.jaerosci.2008.05.007>, 2008.
- 1179
- 1180 Vu, T. V., Shi, Z., Cheng, J., Zhang, Q., He, K., Wang, S., and Harrison, R. M.: Assessing the impact  
1181 of clean air action on air quality trends in Beijing using a machine learning technique, *Atmos. Chem.*  
1182 *Phys.*, 19, 11303–11314, 10.5194/acp-19-11303-2019, 2019.
- 1183
- 1184 Waked, A., Favez, O., Alleman, L. Y., Piot, C., Petit, J. E., Delaunay, T., Verlinden, E., Golly, B.,  
1185 Besombes, J. L., Jaffrezo, J. L., and Leoz-Garziandia, E.: Source apportionment of PM<sub>10</sub> in a north-  
1186 western Europe regional urban background site (Lens, France) using positive matrix factorization and  
1187 including primary biogenic emissions, *Atmos. Chem. Phys.*, 14, 3325–3346, 10.5194/acp-14-3325-  
1188 2014, 2014.
- 1189
- 1190 Wang, G., Gu, S., Chen, J., Wu, X., and Yu, J.: Assessment of health and economic effects by PM<sub>2.5</sub>  
1191 pollution in Beijing: a combined exposure–response and computable general equilibrium analysis,  
1192 *Environ. Technol.*, 37, 3131–3138, 10.1080/09593330.2016.1178332, 2016.
- 1193
- 1194 Wang, L., Zhang, N., Liu, Z., Sun, Y., Ji, D., and Wang, Y.: The Influence of Climate Factors,  
1195 Meteorological Conditions, and boundary-layer structure on severe haze pollution in the Beijing-  
1196 Tianjin-Hebei region during January 2013, *Adv. Meteorol.*, 2014, 685971, 10.1155/2014/685971,  
1197 2014.
- 1198
- 1199 Wang, Y., Hopke, P. K., Xia, X., Rattigan, O. V., Chalupa, D. C., and Utell, M. J.: Source  
1200 apportionment of airborne particulate matter using inorganic and organic species as tracers, *Atmos.*  
1201 *Environ.*, 55, 525–532, 2012.
- 1202



- 1203 Wang, Q., Shao, M., Zhang, Y., Wei, Y., Hu, M., and Guo, S.: Source apportionment of fine organic  
1204 aerosols in Beijing, *Atmos. Chem. Phys.*, 9, 8573-8585, 10.5194/acp-9-8573-2009, 2009.  
1205
- 1206 Wang, H., Zhuang, Y., Wang, Y., Sun, Y., Yuan, H., Zhuang, G., and Hao, Z.: Long-term monitoring  
1207 and source apportionment of PM<sub>2.5</sub>/PM<sub>10</sub> in Beijing, China, *J. Environ. Sci.*, 20, 1323-1327,  
1208 [https://doi.org/10.1016/S1001-0742\(08\)62228-7](https://doi.org/10.1016/S1001-0742(08)62228-7), 2008.  
1209
- 1210 Watson, J. G., Robinson, N. F., Chow, J. C., Henry, R. C., Kim, B., Pace, T., Meyer, E. L., and  
1211 Nguyen, Q.: The USEPA/DRI chemical mass balance receptor model, CMB 7.0, *Environ. Soft.*, 5,  
1212 38-49, 1990.  
1213
- 1214 Wu, X., Chen, C., Vu, T. V., Liu, D., Baldo, C., Shen, X., Zhang, Q., Cen, K., Zheng, M., He, K.,  
1215 Shi, Z., and Harrison, R. M.: Source apportionment of fine organic carbon (OC) using receptor  
1216 modelling at a rural site of Beijing: Insight into seasonal and diurnal variation of source contributions,  
1217 *Environ. Pollut.*, 115078, 2020.  
1218
- 1219 Wu, P., Ding, Y., and Liu, Y. J. A. i. A. S.: Atmospheric circulation and dynamic mechanism for  
1220 persistent haze events in the Beijing–Tianjin–Hebei region, *Adv. Atmos. Sci.*, 34, 429-440, 2017.  
1221
- 1222 Xie, Y., Dai, H., Zhang, Y., Wu, Y., Hanaoka, T., and Masui, T. J. E. i.: Comparison of health and  
1223 economic impacts of PM<sub>2.5</sub> and ozone pollution in China, *Environ. Int.*, 130, 104881,  
1224 <https://doi.org/10.1016/j.envint.2019.05.075>, 2019.  
1225
- 1226 Xing, Y.-F., Xu, Y.-H., Shi, M.-H., and Lian, Y.-X.: The impact of PM<sub>2.5</sub> on the human respiratory  
1227 system, *J. Thorac. Dis.*, 8, E69-E74, 10.3978/j.issn.2072-1439.2016.01.19, 2016.
- 1228 Xu, J., Liu, D., Wu, X., Vu, T., V., Zhang, Y., Fu, P., Sun, Y., Harrison, R., M., and Shi, Z.: Source  
1229 apportionment of fine aerosol at an urban site of Beijing using a chemical mass balance model in  
1230 preparation, *Atmos. Chem. Phys. Discuss.*, <https://doi.org/10.5194/acp-2020-1020>, in review, 2020 .  
1231
- 1232 Xu, W., Sun, Y., Wang, Q., Zhao, J., Wang, J., Ge, X., Xie, C., Zhou, W., Du, W., Li, J., Fu, P.,  
1233 Wang, Z., Worsnop, D. R., and Coe, H.: Changes in aerosol chemistry from 2014 to 2016 in winter  
1234 in Beijing: Insights from high-resolution aerosol mass spectrometry, *J. Geophys. Res.-Atmos.*, 124,  
1235 1132-1147, 10.1029/2018JD029245, 2019.  
1236
- 1237 Yan, C., Zheng, M., Sullivan, A. P., Shen, G., Chen, Y., Wang, S., Zhao, B., Cai, S., Desyaterik, Y.,  
1238 Li, X., Zhou, T., Gustafsson, Ö., and Collett, J. L.: Residential coal combustion as a source of  
1239 levoglucosan in China, *Environ. Sci. Technol.*, 52, 1665-1674, 10.1021/acs.est.7b05858, 2018.  
1240
- 1241 Yu, L., Wang, G., Zhang, R., Zhang, L., Song, Y., Wu, B., Li, X., An, K., and Chu, J.:  
1242 Characterization and source apportionment of PM<sub>2.5</sub> in an urban environment in Beijing, *Aerosol Air  
1243 Qual. Res.*, 13, 574-583, 10.4209/aaqr.2012.07.0192, 2013.  
1244
- 1245 Zhang, Y., Ren, H., Sun, Y., Cao, F., Chang, Y., Liu, S., Lee, X., Agrios, K., Kawamura, K., Liu, D.,  
1246 Ren, L., Du, W., Wang, Z., Prévôt, A. S. H., Szidat, S., and Fu, P.: High contribution of nonfossil  
1247 sources to submicrometer organic aerosols in Beijing, China, *Environ. Sci. Technol.*, 51, 7842-7852,  
1248 10.1021/acs.est.7b01517, 2017.  
1249
- 1250 Zhang, J. K., Cheng, M. T., Ji, D. S., Liu, Z. R., Hu, B., Sun, Y., and Wang, Y. S.: Characterization  
1251 of submicron particles during biomass burning and coal combustion periods in Beijing, China, *Sci.  
1252 Tot. Environ.*, 562, 812-821, <https://doi.org/10.1016/j.scitotenv.2016.04.015>, 2016.  
1253



- 1254 Zhang, J.-J., Cui, M.-M., Fan, D., Zhang, D.-S., Lian, H.-X., Yin, Z.-Y., and Li, J.: Relationship  
1255 between haze and acute cardiovascular, cerebrovascular, and respiratory diseases in Beijing,  
1256 *Environ. Sci. Pollut. Res.*, 22, 3920-3925, 10.1007/s11356-014-3644-7, 2015a.  
1257
- 1258 Zhang, J., Wang, Y., Huang, X., Liu, Z., Ji, D., and Sun, Y.: Characterization of organic aerosols in  
1259 Beijing using an aerodyne high-resolution aerosol mass spectrometer, *Adv. Atmos. Sci.*, 32, 877-888,  
1260 10.1007/s00376-014-4153-9, 2015b.  
1261
- 1262 Zhang, J. K., Sun, Y., Liu, Z. R., Ji, D. S., Hu, B., Liu, Q., and Wang, Y. S.: Characterization of  
1263 submicron aerosols during a month of serious pollution in Beijing, 2013, *Atmos. Chem. Phys.*, 14,  
1264 2887-2903, 10.5194/acp-14-2887-2014, 2014.  
1265
- 1266 Zhang, Y., Sun, J., Zhang, X., Shen, X., Wang, T., and Qin, M.: Seasonal characterization of  
1267 components and size distributions for submicron aerosols in Beijing, *Sci. China Earth Sci.*, 56, 890-  
1268 900, 10.1007/s11430-012-4515-z, 2013.  
1269
- 1270 Zhang, X., Hecobian, A., Zheng, M., Frank, N. H., and Weber, R. J.: Biomass burning impact on  
1271 PM<sub>2.5</sub> over the southeastern US during 2007: integrating chemically speciated FRM filter  
1272 measurements, MODIS fire counts and PMF analysis, *Atmos. Chem. Phys.*, 10, 6839-6853,  
1273 10.5194/acp-10-6839-2010, 2010.  
1274
- 1275 Zhang, Y., Sheesley, R. J., Schauer, J. J., Lewandowski, M., Jaoui, M., Offenber, J. H., Kleindienst,  
1276 T. E., and Edney, E. O.: Source apportionment of primary and secondary organic aerosols using  
1277 positive matrix factorization (PMF) of molecular markers, *Atmos. Environ.*, 43, 5567-5574, 2009.  
1278
- 1279 Zhang, Y., Schauer, J. J., Zhang, Y., Zeng, L., Wei, Y., Liu, Y., and Shao, M.: Characteristics of  
1280 particulate carbon emissions from real-world Chinese coal combustion, *Environ. Sci. Technol.*, 42,  
1281 5068-5073, 10.1021/es7022576, 2008.  
1282
- 1283 Zhang, Y.-x., Min, S., Zhang, Y.-h., Zeng, L.-m., He, L.-y., Bin, Z., Wei, Y.-j., and Zhu, X.-l.: Source  
1284 profiles of particulate organic matters emitted from cereal straw burnings, *Journal of Environmental  
1285 Sciences*, 19, 167-175, 2007.  
1286
- 1287 Zhao, Z.-Y., Cao, F., Fan, M.-Y., Zhang, W.-Q., Zhai, X.-Y., Wang, Q., and Zhang, Y.-L. J. A. E.:  
1288 Coal and biomass burning as major emissions of NO<sub>x</sub> in Northeast China: Implication from dual  
1289 isotopes analysis of fine nitrate aerosols, *Atmos. Environ.*, 242, 117762, 2020.  
1290
- 1291 Zhao, X., Hu, Q., Wang, X., Ding, X., He, Q., Zhang, Z., Shen, R., Lü, S., Liu, T., Fu, X., and Chen,  
1292 L.: Composition profiles of organic aerosols from Chinese residential cooking: case study in urban  
1293 Guangzhou, south China, *J. Atmos. Chem.*, 72, 1-18, 10.1007/s10874-015-9298-0, 2015.
- 1294 Zheng, M., Salmon, L. G., Schauer, J. J., Zeng, L., Kiang, C. S., Zhang, Y., and Cass, G. R.: Seasonal  
1295 trends in PM<sub>2.5</sub> source contributions in Beijing, China, *Atmos. Environ.*, 39, 3967-3976,  
1296 <https://doi.org/10.1016/j.atmosenv.2005.03.036>, 2005.  
1297
- 1298 Zhou, Y., Zheng, N., Luo, L., Zhao, J., Qu, L., Guan, H., Xiao, H., Zhang, Z., Tian, J., and Xiao, H.:  
1299 Biomass burning related ammonia emissions promoted a self-amplifying loop in the urban  
1300 environment in Kunming (SW China), *Atmos. Environ.*, 118138,  
1301 <https://doi.org/10.1016/j.atmosenv.2020.118138>, 2020.  
1302



1303 **TABLE LEGENDS**

1304 **Table 1.** List of the studies conducted in the Beijing metropolitan area to evaluate PM sources.

1305

1306 **FIGURE LEGENDS**

1307 **Figure 1.** Factor profiles for identified factors at IAP and PG. The bars show the composition  
1308 profile (left axis) and the dots, the Explained Variation (right axis).

1309 **Figure 2.** Temporal variation of identified factors at IAP and PG. Solid and broken lines represent  
1310 IAP and PG, respectively.

1311 **Figure 3.** Contribution of different sources to PM<sub>2.5</sub> mass at IAP and PG.

1312 **Figure 4.** Correlations observed between PMF and CMB results at IAP. \*If two outlying points  
1313 are removed from the coal combustion-PMF, correlations are markedly improved.

1314 **Figure 5.** Correlations observed between PMF and CMB results at PG.

1315 **Figure 6.** Correlations observed between PMF and online AMS PMF results at IAP (winter). \*If  
1316 two outlying points are removed from the coal combustion-PMF, correlations are  
1317 markedly improved.

1318 **Figure 7.** Correlations observed between PMF and offline AMS PMF results at IAP (winter).

1319

1320



1321 **Table 1.** List of the studies conducted in the Beijing metropolitan area to evaluate PM sources.

1322

Reported Studies	PM size fraction	Sampling site	Study period	Identified PMF factors (% contribution)						Input species
				Dust/soil dust <sup>a</sup> /road dust <sup>b</sup> /mineral dust <sup>c</sup> /local <sup>b</sup> /non-local <sup>d</sup>	Traffic/fossil fuel <sup>e</sup>	Coal combustion	Biomass burning	Secondary inorganics	Industrial	
Li et al. (2019)	PM <sub>2.5</sub>	Urban- IAP	15 <sup>th</sup> Sep – 12 <sup>th</sup> Nov 2014	-	-	-	-	-	-	Mg, Al, K, Ca and Fe, V, Cr, Mn, Co, Cu, Zn, Ag, Cd, Pb and As
		Suburban-UCAS	15 <sup>th</sup> Sep – 12 <sup>th</sup> Nov 2014	-	-	-	-	-	-	
Liu et al. (2019)	PM <sub>2.5</sub>	PKU	Nov-Dec 2016	5	18	16	9	44	8	OC, EC, NO <sub>3</sub> <sup>-</sup> , SO <sub>4</sub> <sup>2-</sup> , NH <sub>4</sub> <sup>+</sup> , Cl <sup>-</sup> , Na <sup>+</sup> , Mg, Al, K, Ca, Ba, Cr, Mn, Fe, Ni, Cu, Zn, As, Se, and Pb
Ma et al. (2017a)	PM <sub>2.5</sub>	Urban- IAP	24 <sup>th</sup> Feb - 12 <sup>th</sup> Mar 2014	10*	6	18 <sup>e</sup>	18 <sup>e</sup>	46	20	Na <sup>+</sup> , K <sup>+</sup> , Mg <sup>2+</sup> , Ca <sup>2+</sup> , NO <sub>3</sub> <sup>-</sup> , SO <sub>4</sub> <sup>2-</sup> , NH <sub>4</sub> <sup>+</sup> , Cl <sup>-</sup> , Al, Fe, Ti, Mn, Cu, Zn, Sb, Pb, Cr, PM <sub>2.5</sub> , EC, OC
Tian et al. (2016)	PM <sub>2.1</sub>	Urban- IAP	Mar 2013 – 28 <sup>th</sup> Feb 2014	8.4 <sup>s</sup>	19.6	17.7	11.1	25.1	12.1	Na, Mg, Al, K, Ca, Mn, Fe, Co, Ni, Cu, Zn, Mo, Cd, Ba, Ti, Pb, Th, U, Na <sup>+</sup> , NH <sub>4</sub> <sup>+</sup> , K <sup>+</sup> , Mg <sup>2+</sup> , Ca <sup>2+</sup> , Cl <sup>-</sup> , SO <sub>4</sub> <sup>2-</sup> , NO <sub>3</sub> <sup>-</sup> , OC and EC.
	PM <sub>2.1-9</sub>		Mar 2013 – 28 <sup>th</sup> Feb 2014	10.9 <sup>s</sup> , 22.6 <sup>a</sup>	-	7.8	11.8	9.8	5.1	
Yu et al. (2013)	PM <sub>2.5</sub>	Urban-BNU	1 <sup>st</sup> Jan – 31 <sup>st</sup> Dec 2010	12.7 <sup>s</sup> , 10.4*	17.1, 16 <sup>c</sup>		11.2	26.5 <sup>e</sup>	6	Mg, Al, Si, P, S, Cl, K, Ca, Ti, V, Cr, Mn, Fe, Ni, Cu, Zn, As, Se, Br, Ba and Pb
Zhang et al. (2013)	PM <sub>2.5</sub>	PKU	April, July, Oct 2009 and Jan 2010	16*	3 <sup>+</sup>	14	13	26	28	Na <sup>+</sup> , K <sup>+</sup> , Mg <sup>2+</sup> , Ca <sup>2+</sup> , NO <sub>3</sub> <sup>-</sup> , SO <sub>4</sub> <sup>2-</sup> , NH <sub>4</sub> <sup>+</sup> , Cl <sup>-</sup> , Al, Fe, Na, Mg, K, Ca, Ba, Co, Mo, Cd, Sn, As, Se, Rb, Ti, Mn, Cu, Zn, Sb, Pb, Cr, PM <sub>2.5</sub> , EC, OC
Wang et al. (2008)	PM <sub>2.5</sub>	Urban-BNU	Summer and winter	8.8 <sup>b</sup> , 6.7 <sup>c</sup>	5.9	16.7	11.8	12.7 <sup>t</sup> , 14.7 <sup>z</sup>	8.8	Na, K <sup>+</sup> , Mg <sup>2+</sup> , NO <sub>3</sub> <sup>-</sup> , SO <sub>4</sub> <sup>2-</sup> , NH <sub>4</sub> <sup>+</sup> , Cl <sup>-</sup>



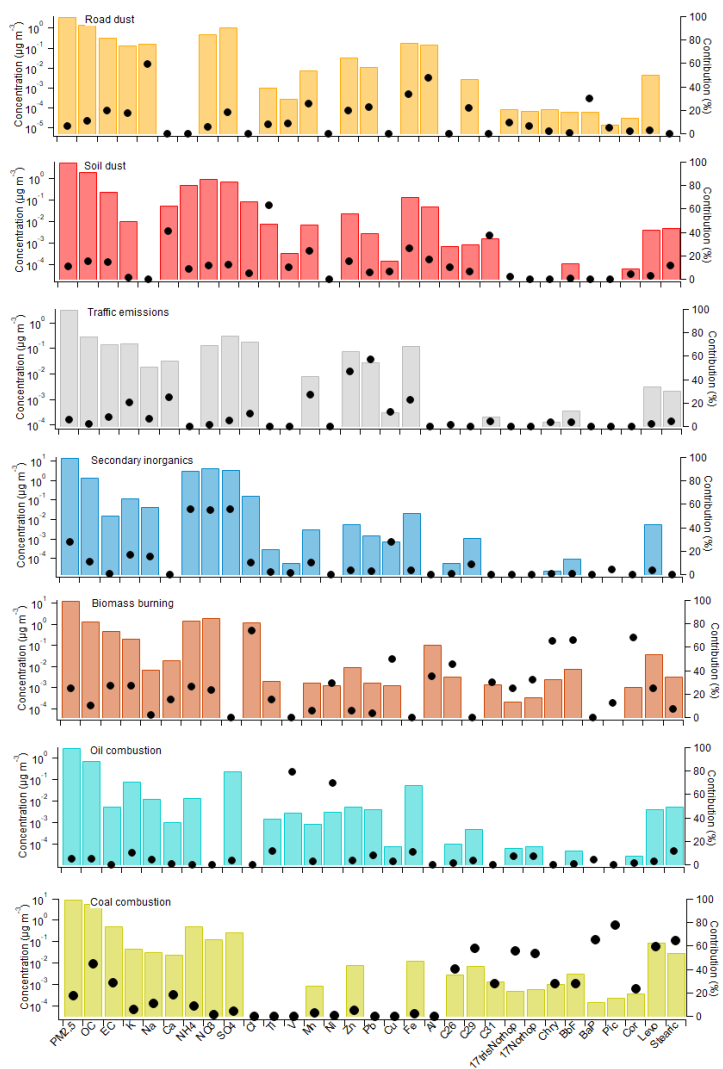
	PM <sub>10</sub>		2001 to 2006 Summer and winter 2001 to 2006	23 <sup>β</sup>	8.4	13.3	10.2	18.9	14.9	Al, Fe, Na, Mg, K, Ca, Co, Cd, As, Ti, Mn, Cu, Zn, Sb, Pb, S, Cr, BC, OC, C <sub>2</sub> O <sub>4</sub> <sup>2-</sup>
	PM <sub>2.5</sub>	Duolun <sup>Ⓢ</sup>	Summer and winter 2001 to 2006	36.2 <sup>β</sup> , 23.1 <sup>Ⓢ</sup>	-	-	15.6	7.1 <sup>†</sup>	-	
	PM <sub>10</sub>		Summer and winter 2001 to 2006	61.7 <sup>β</sup> , 11 <sup>Ⓢ</sup>	-	-	18.1	4.1	-	
Song et al. (2007)	PM <sub>2.5</sub>	Urban-PKU, OLC, SJS, TZ, and LX; Rural-MT	Jan 2004	7.8 <sup>Ⓢ</sup>	8.5	40.6	16.4	9.2 <sup>‡</sup> , 10.5 <sup>‡</sup>	-	OC, EC, NO <sub>3</sub> <sup>-</sup> , SO <sub>4</sub> <sup>2-</sup> , NH <sub>4</sub> <sup>+</sup> , Cl <sup>-</sup> , Na, Mg, Al, K, Ca, Ti, V, Cr, Mn, Fe, Ni, Cu, Zn, As, Se, and Pb
			Aug 2004	4.4 <sup>Ⓢ</sup>	7.8	5.9	6.7	12.6 <sup>‡</sup> , 4.2 <sup>‡</sup>	-	
Song et al. (2006)	PM <sub>2.5</sub>	OT, NB, BJ, XY, CH	6-day intervals in Jan, Apr, Jul, and Oct 2000	9 <sup>Ⓢ</sup> and yellow dust	6	19	11	17 <sup>‡</sup> , 14 <sup>‡</sup>	6	OC, EC, NO <sub>3</sub> <sup>-</sup> , SO <sub>4</sub> <sup>2-</sup> , NH <sub>4</sub> <sup>+</sup> , Na, Al, Si, Cl, K, Ca, Ti, V, Cr, Mn, Fe, Ni, Cu, Zn, As, Se, Br, Pb, and Mg

1323 <sup>†</sup> Reported as traffic and waste incineration emissions; <sup>‡</sup> Secondary sulphur/<sup>‡</sup> secondary nitrate; <sup>Ⓢ</sup> Fossil  
 1324 fuel; <sup>‡</sup> Reported as combined coal and biomass burning contribution; <sup>Ⓢ</sup> Background site; University  
 1325 of Chinese Academy of Sciences-UCAS; Peking University-PKU; Beijing Normal University-BNU;  
 1326 Ming Tombs -OT, the airport-NB, Beijing University-BJ, Dong Si EPB-XY, and Yong Le Dian-CH

1327



1328

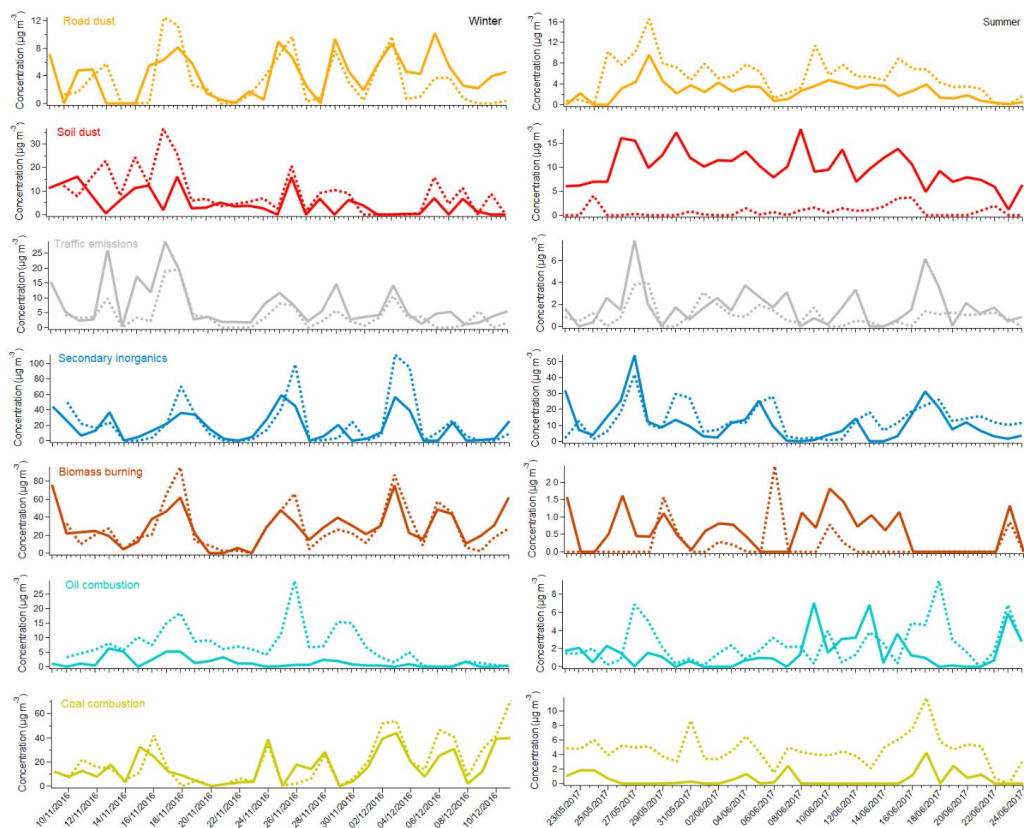


1329

1330 **Figure 1.** Factor profiles for identified factors at IAP and PG. The bars show the composition profile  
1331 (left axis) and the dots, the Explained Variation (right axis).

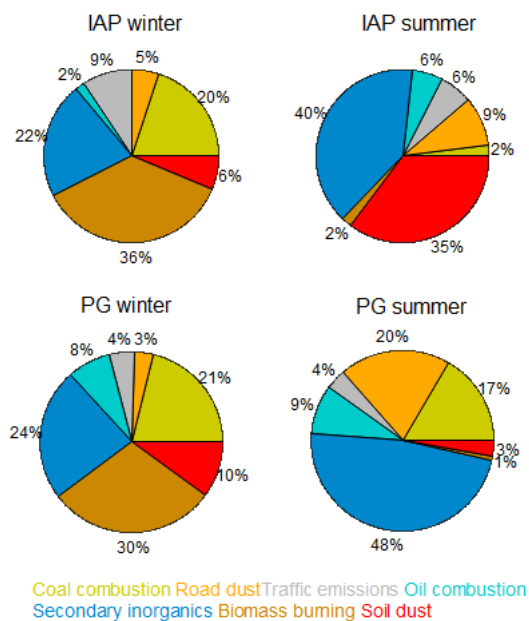
1332

1333



1334

1335 **Figure 2.** Temporal variation of identified factors at IAP and PG. Solid and broken lines represent  
1336 IAP and PG, respectively.  
1337



1338

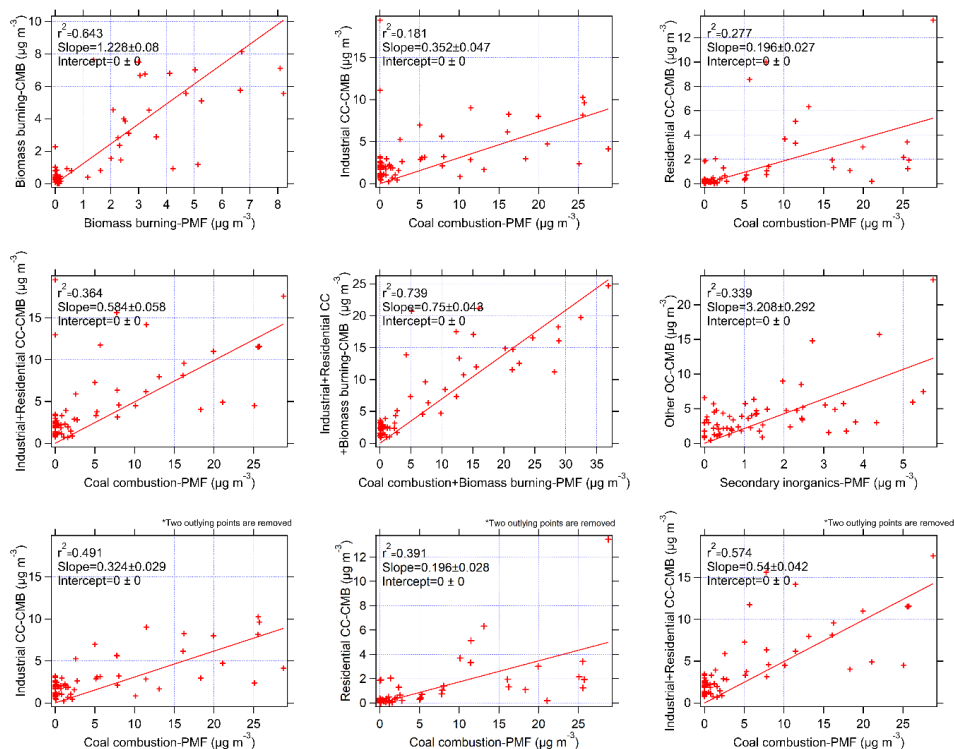
1339 **Figure 3.** Contribution of different sources to PM<sub>2.5</sub> mass at IAP and PG.

1340



1341

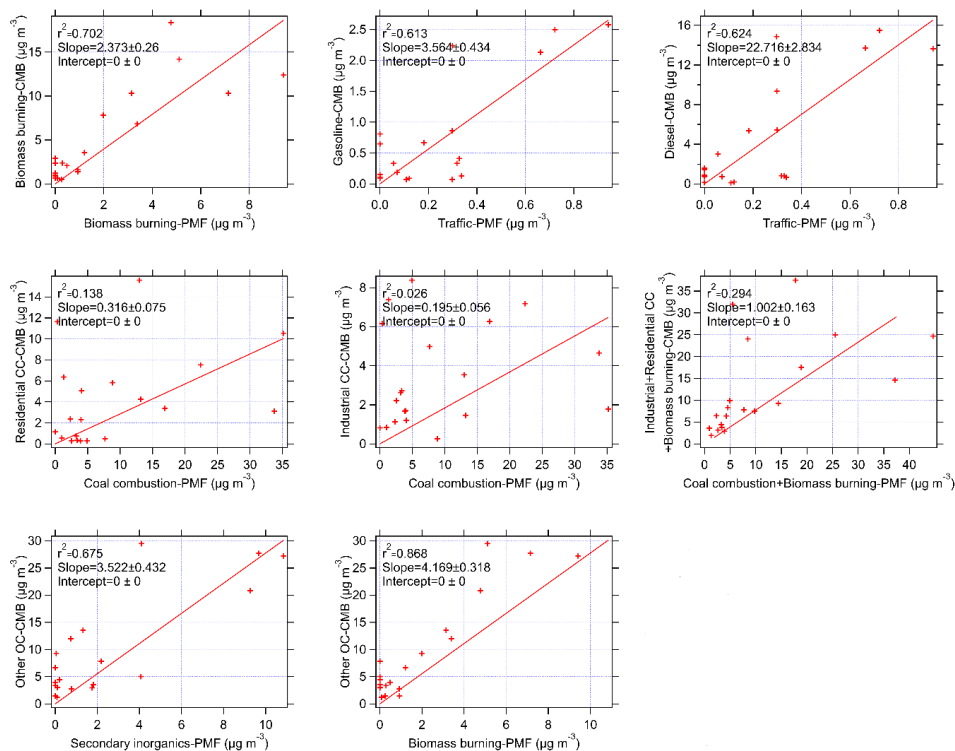
1342



1343

1344 **Figure 4.** Correlations observed between PMF and CMB results at IAP. \*If two outlying points are  
1345 removed from the coal combustion-PMF, correlations are markedly improved.

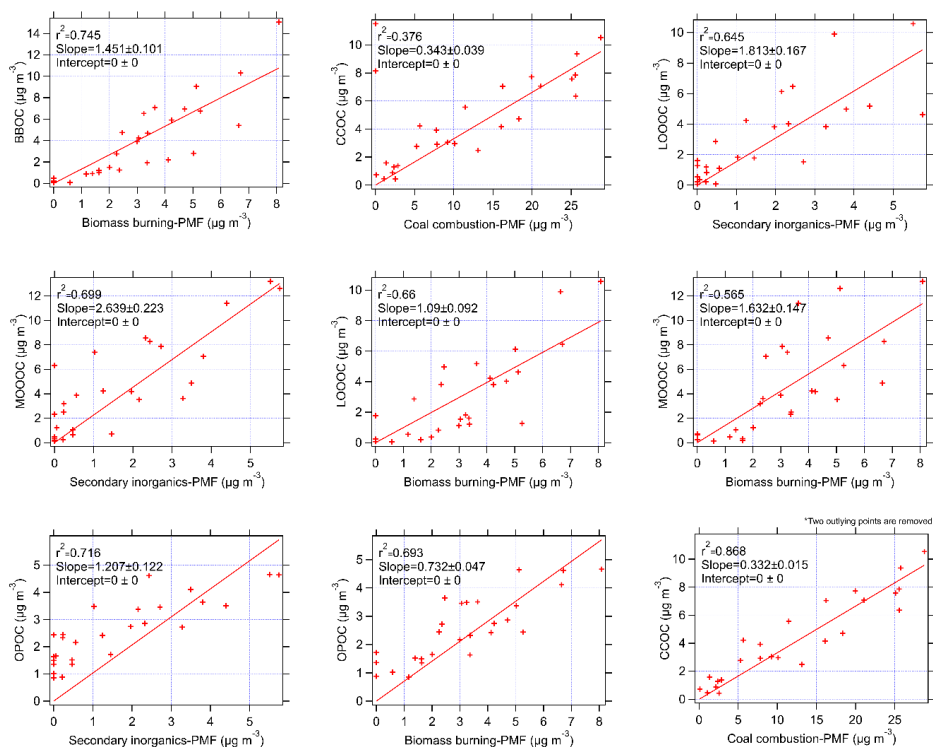
1346



1347

1348 **Figure 5.** Correlations observed between PMF and CMB results at PG.

1349

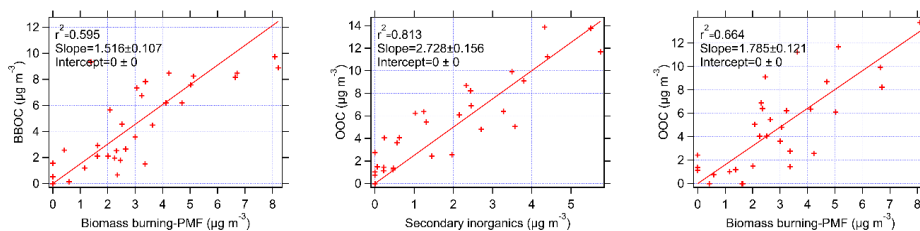


1350

1351 **Figure 6.** Correlations observed between PMF and online AMS PMF results at IAP (winter). \*If two  
 1352 outlying points are removed from the coal combustion-PMF, correlations are markedly improved.  
 1353



1354



1355

1356 **Figure 7.** Correlations observed between PMF and offline AMS PMF results at IAP (winter).

1357

1358